REVIEW

Check for updates

Organelle-targeting ratiometric fluorescent probes: design principles, detection mechanisms, bio-applications, and challenges

Manoj Kumar Goshisht, [iD] ab Neetu Tripathi, [iD] *c Goutam Kumar Patra [iD] d and Manohar Chaskar [iD] e

Biological species, including reactive oxygen species (ROS), reactive sulfur species (RSS), reactive nitrogen species (RNS), F⁻, Pd²⁺, Cu²⁺, Hg²⁺, and others, are crucial for the healthy functioning of cells in living organisms. However, their aberrant concentration can result in various serious diseases. Therefore, it is essential to monitor biological species in cellular organelles such as the cell membrane, mitochondria, lysosome, endoplasmic reticulum, Golgi apparatus, and nucleus. Among various fluorescent probes for species detection within the organelles, ratiometric fluorescent probes have drawn special attention as a potential way to get beyond the drawbacks of intensity-based probes. This method depends on measuring the intensity change of two emission bands (caused by an analyte), which produces an efficient

aDepartment of Chemistry, Natural and Applied Sciences, University of Wisconsin—Green Bay, 2420 Nicolet Drive, Green Bay, WI, 54311-7001, USA. E-mail: Kumarm@uwgb.edu

bDepartment of Chemistry, Government Naveen College Tokapal, Bastar, Chhattisgarh, 494442, India. E-mail: mkgh07@gmail.com

cDepartment of Chemistry, Guru Nanak Dev University, Amritsar, Punjab, 143005, India. E-mail: neetutripathi1990@yahoo.com; neetuchem1990@gmail.com

dDepartment of Chemistry, Faculty of Physical Sciences, Guru Ghasidas Vishwavidyalaya, Bilaspur, Chhattisgarh, 495009, India. E-mail: patragoutam137@gmail.com

eDepartment of Technology, Savitribai Phule Pune University, Ganeshkhind, Pune, 411007, India. E-mail: chaskarmanohar@gmail.com

Dr Manoj Kumar Goshisht is an Assistant Professor of Chemistry at Govt Naveen College Tokapal, Bastar, Chhattisgarh, India. He obtained his masters degree from Guru Jambheshwar University of Science & Technology, Hisar, Haryana, and PhD degree from Dr B. R. Ambedkar National Institute of Technology, Jalandhar, Punjab, India. He has cleared the National Eligibility Test (CSIR-UGC NET) for Assistant Professor in the subject of Chemical Sciences. He is a winner of the Editors Pick Award of the ''9th DST & ACS Workshop.'' Currently, he is a visiting scientist at University of Wisconsin—Green Bay, USA. His research interests include organic chemistry, materials chemistry, supramolecular chemistry, and nanomaterials. He has published various research papers in reputed international peer-reviewed journals of The American Chemical Society, The Royal Society of Chemistry, and Springer Nature. He also has a book to his credit published by CRC Press (an imprint of the Taylor & Francis group).

Dr Neetu Tripathi obtained her PhD from Guru Nanak Dev University, Amritsar, India. She completed her masters with 1st rank (Gold medal) in MSc Chemistry (Instrumental Analysis). She has been a recipient of the prestigious INSPIRE fellowship of the Government of India during her PhD She has also cleared the National Eligibility Test for Assistant Professor (CSIR-UGC NET) and the Graduate Aptitude test (GATE) in the subject of chemical sciences. Her research interest includes organic chemistry, materials chemistry, supramolecular chemistry, and nanomaterials. She has published various research papers in international peer-reviewed journals (Royal Society of Chemistry, Elsevier journals and Springer journal). She is also an author of a book published by CRC press (an imprint of the Taylor & Francis group).

internal referencing that increases the detection's sensitivity. This review article discusses the literature publications (from 2015 to 2022) on organelle-targeting ratiometric fluorescent probes, the general strategies, the detecting mechanisms, the broad scope, and the challenges currently faced by fluorescent probes.

1   Introduction

In this modern era, everyone is interconnected. Similarly, in living beings, cells, organelles and biological species are interconnected and act cooperatively for the normal functioning of living systems.[1,2] For instance, biological species (anions, cations, thiols, nitrogen and oxygen) perform a variety of role in organelles such as signaling molecules, enzyme cofactors, *etc.* However, their chemical imbalance can cause cellular malfunction.[3] Therefore, smart research work on organelles and biological species is essential, which is challenging.

Over the years, significant studies and research work have been done on organelles and biological species present within the organelles. For example, organelle-targeting medicine has been developed for curing various diaeases.[4,5] Bioimaging technique has been developed for examining biomolecules in living cells and tissues.[6] Choi *et al.* studied fluorescent probes for organelles with respect to recent advances and bio-applications.[7]

Nowadays, fluorescent probes for targeting organelles have gained more attention due to their excellent photo-physical characteristics, high sensitivity, rapid response, low cost, non-

invasiveness, and real-time imaging.[8] Notably, many single emission probes are unable to withstand environmental interference. Through a built-in correction of two emissions at different wavelengths, ratiometric fluorescence probes could eliminate background interference.[9] Additionally, ratiometric fluorescence imaging has an even better resolution due to the two clearly defined emission peaks.[10] Therefore, the development of ratiometric fluorescent probes is a winning strategy for the sensitive detection of small molecules, thanks to its reduced environmental effect.

Although there are several outstanding reviews in the literature based on ratiometric probes with sensing applications, each one has concentrated on a single aspect, such as the optical processes, a particular class of fluorophores, or a specific subset of target analytes. In 2018, Huang *et al.* reported ratiometric optical nanoprobes for molecular detection and imaging.[10] In an excellent review, the design principles and applications of fluorescent probes in the ratiometric detection of anions, cations, and biological molecules has been beautifully demonstrated.[11] Another review article highlighted various chemo/probe-based semiconductor quantum dots (QDs).[12]

Prof. Goutam Kumar Patra, Head of the Department of Chemistry, Guru Ghasidas Central University, Bilaspur did PhD from Jadavpur University, under the supervision of Prof. Dipankar Datta at Indian Association for the Cultivation of Science, Kolkata. Then he joined the Tel Aviv University, Israel, as a postdoctoral research fellow with Prof. Israel Goldberg (2000–2002). Subsequently he moved to the Carnegie Mellon University, USA where he worked with Prof. Catalina Achim. Successively he joined as Asst. Prof. in Vijoygarh Jyotish Ray College, Kolkata in December 2003. He visited Max Planck Institute of Bioinorganic Chemistry, Mülheim, Germany as a BOYSCAST fellow during 2006–07 and worked in the group of the then Director, Prof. Karl Wieghardt. He has been a Professor in Guru Ghasidas Central University, Bilaspur since 2012 and former Dean, School of Physical Science. His research interests include chemosensors, redox activity, aza macrocyclic chemistry, crystal engineering, porphyrin and supramolecular chemistry, peptide nucleic acids (PNAs) and free radical chemistry. So far, he has published more than hundred research papers in journals of national and international repute and guided eight doctoral students and one post-doctoral student.

Dr Manohar Chaskar is the Dean of the Science and Technology Faulty of Savitribai Phule Pune University. Dr Chaskar completed his PhD in materials science, and his post-doc from Nagoya University, Japan in photocatalysis. Dr Chaskar's research interests include the use of nanomaterials in catalyzing organic reactions. Dr Chaskar has published several high impact research articles in reputed national and international journals and has one patent to his credit while two are in the process. He is also a visiting scientist in Germany and Japan.

In 2020, Wu *et al.* summarized recent advancements in the metal–organic framework (MOF)-based ratiometric fluorescent probes.[13] Recently, Bigdeli *et al.* published a review article on fluorescent nanoprobes for visual detection.[8]

We illustrate the design principles, fundamental detection mechanisms, and applications of organelle-targeting ratiometric fluorescent probes. The current limitations and prospective future directions, which would spur additional research interest and bring up fresh opportunities for biological analysis, are also covered.

2 Design principles

In designing fluorescent probes, photo-physical parameters such as photo-induced electron transfer (PET), internal charge transfer (ICT), monomer–excimer formation, Förster resonance energy transfer (FRET), and excited state intramolecular proton transfer (ESIPT) are frequently used. FRET is a relatively excellent strategy for designing ratiometric fluorescent probes and increasing the Stokes shift.[14]

Generally, the design of ratiometric probes involves the combination of two fluorophores, one reference fluorophore (may or may not show a change in emission intensity upon interaction with the analyte) and another dynamic fluorophore (always shows a change in emission intensity upon interaction with the analyte).[8] Generally, ratiometric changes in the emission spectrum are of the following type:

(I) Static + dynamic change: herein, upon the addition of an analyte, the emission intensity of one fluorophore is almost kept unchanged, whereas other fluorophores may undergo an increase/decrease/shift in emission intensity (Fig. 1A).[15,16]

(II) Dynamic + dynamic change: herein, both the fluorophores change (increase/decrease/or shift in emission intensity), but in opposite directions (Fig. 1B).[17]

Generally, organelle-targeting ratiometric fluorescent probes contain a fluorophore, recognition units, and targeting moieties (Fig. 2). The organelle-targeting groups are selective to specific organelles. For example, due to its alkalinity, the morpholine group is a conventional lysosome-targeting moiety.[18] In addition, the polarity-dependent approach helps create various biological probes, which are helpful for imaging multiple organelles.[19]
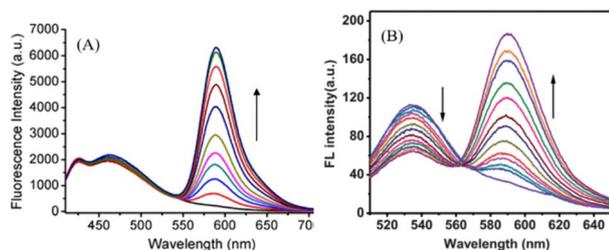

Fig. 1 Schematic representation of the ratiometric fluorescence change when (A) static + dynamic fluorophores (reprinted from ref. 15, copyright 2019, Elsevier) and (B) dynamic + dynamic fluorophores (reprinted from ref. 17, copyright 2012, The Royal Society of Chemistry) are utilized.

2.1 Designing mitochondria-targeting ratiometric fluorescent probes

Since the mitochondrial membrane typically has a potential of -180 mV, this property is employed to direct lipophilic positively charged probes into the mitochondria.[20] The common mitochondrial-targeting units include the quaternized pyridine moiety,[21] triphenylphosphonium (TPP),[22,23] indole,[24] cyanine,[25,26] pyridinium,[27,28] and rhodamine[29] (Fig. 2a).[30–33] Furthermore, to ascertain the mitochondria localization of probes in cells, the co-localization experiment was performed using commercially available mitochondrion-specific dyes such as MitoTracker Green FM, MitoTracker Red, and MitoTracker Orange.[30] Generally, mitochondrion-targeting fluorescent probes consist of a fluorophore linked to the mitochondrion-targeting moiety and an activation unit.

2.2 Designing lysosome-targeting ratiometric fluorescent probes

Modifying them with lipophilic amines is the most popular method for directing probes into lysosomes.[34–36] Due to the membrane-impermeable protonated amines in lysosomes, selective probe trapping occurs. The pyridine group,[37] monothio-bishydrazide moiety,[14] and morpholine[15] are the common lysosome-targeting groups (Fig. 2b). Typically, the design of the probe for lysosome requires linking of the fluorophore with the lysosome-targeting group and an activation unit.

2.3 Designing endoplasmic reticulum-targeting ratiometric fluorescent probes

The commonly used ER-targeting moieties include glibenclamide,[38] methyl sulphonamide,[39] and the *p*-toluenesulfonamide group (Fig. 2c).[40,41] ER-targeting fluorescent probes generally have (1) a moderate size (conjugated band numbers (CBN < 40)), (2) a cationic character, and (3) an appropriate lipophilicity ($+6 > \log P_{oct} > 0$).[42] The ER-targeting fluorescent probes mainly track cellular concentrations of stress-responsive substances like NO, H_2S, H_2O_2, and HOCl.[43,44]

2.4 Designing Golgi-apparatus-targeting ratiometric fluorescent probes

Motivated by the abundance of cysteine residues in the Golgi apparatus, Huang and coworkers proved L-cysteine as an effective Golgi apparatus targeting ligand. They created various probes using this technique (Fig. 2d).[45–48]

2.5 Designing nucleus-targeting ratiometric fluorescent probes

The nuclear envelope is a highly controlled membrane barrier. Therefore, passive diffusion or active transport uses the nuclear pore complex (NPC) to target the nucleus.[49] Small fluorescent probes with cationic centers and hydrophobic planar aromatic structures can selectively label DNA molecules by focusing on the minor grooves in DNA (negatively charged double strands). Some of them have been made available for purchase.[50,51] From a molecular docking experiment, Ma *et al.* demonstrated
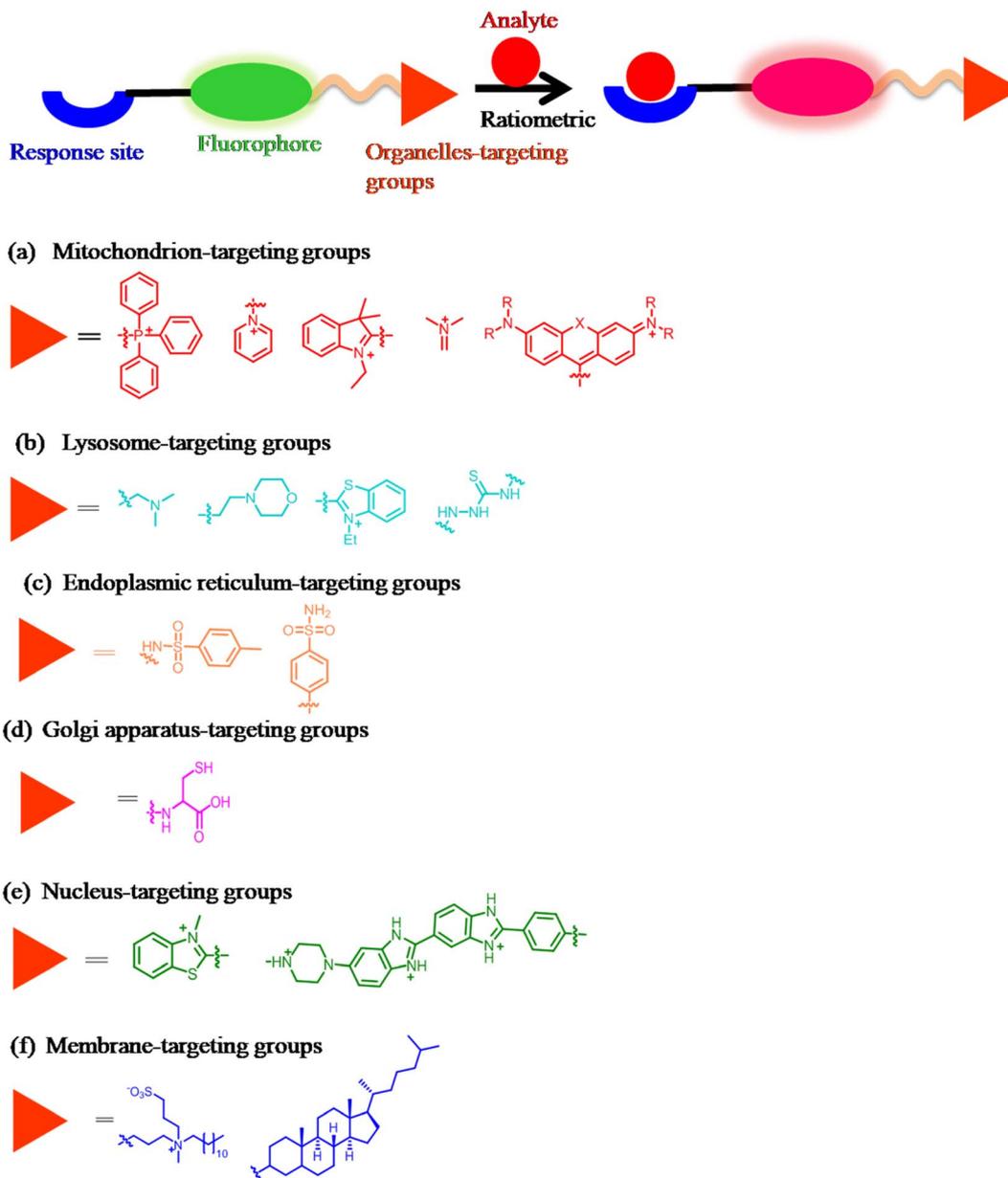
Fig. 2 General strategies for designing organelle-targeting ratiometric fluorescent probes and common organelle-targeting groups for (a) mitochondria; (b) lysosome; (c) endoplasmic reticulum; (d) Golgi apparatus; (e) nucleus; (f) membrane.

electrostatic binding between a positively charged probe and negatively charged nucleus RNA major groove (affinity energy = -5.78 kcal mol^{-1}).[52] Nucleus-targeting unit functionalization is an excellent strategy for delivering fluorescent functional probes into the nucleus of living cells (Fig. 2e).[53,54]

2.6 Designing membrane-targeting ratiometric fluorescent probes

Currently, the available probes for the membrane share a common approach: the conjugation of an environment-sensitive fluorophore to generate membrane-specific signals and a membrane-anchoring moiety to minimize the diffusion of the probe (Fig. 2f).[7]

3 Detection mechanism

The various fluorescence-based sensing mechanisms include photo-induced electron transfer (PET), internal charge transfer (ICT), monomer–excimer formation, Förster resonance energy transfer (FRET), and excited state intra-molecular proton transfer (ESIPT). These mechanisms are available in detail in our recent publications[55–57] and some excellent reviews.[9,58] In this section, we explain the fluorescence-based sensing mechanisms briefly. The HOMO localizes on the donor moieties in the ICT-based fluorescent probe. The LUMO is centered on acceptor moieties, thus creating a solid dipole with a charge transfer phenomenon upon excitation. The preferential interaction of the analyte at
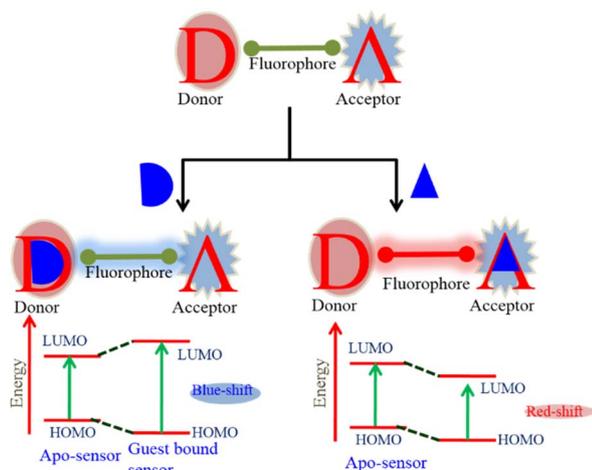
Fig. 3 Schematic representation of the internal charge transfer (ICT)-based sensing mechanism in ratiometric design.

either the donor or acceptor results in a change in dipole strengths and, consequently, spectral shifts (Fig. 3). To effectively measure ratiometrically, an ICT-based probe should exhibit a visible difference in fluorescence intensity as well as a significant change in emission wavelength. In the PET process (Fig. 4), upon excitation, an electron is transferred from the HOMO

(highest occupied molecular orbital) of the receptor (donor) to the LUMO (lowest unoccupied molecular orbital) of the fluorophore (acceptor). However, in the case of the guest-bounded receptor, the HOMO energy levels become lower than those of the fluorophore, inhibiting the PET process and fluorescence change. In the monomer–excimer-based sensing mechanism, upon the addition of an analyte, generally excited state complex formation (excimer) occurs by the interaction between the excited states of one fluorophore and the ground state of another molecule (Fig. 5). The probes that include polyaromatic hydrocarbon (PAH) moieties, such as pyrene, anthracene, etc., typically display this type of sensing mechanism. In the FRET process, energy is transferred from the excited donor molecule to the ground-state acceptor molecule. The critical parameter which governs the FRET phenomenon is spectral overlaps (donor emission spectrum and acceptor absorption spectrum) (Fig. 6). FRET-based probes prove to be an excellent tool for ratiometric imaging due to the stoichiometric relationship between the donor (D) and acceptor (A). In the ESIPT process, proton transfer occurs from the preferred enol-form to the excited state keto-form upon excitation. During relaxation, the excited state keto-form converts back to the enol form by reverse proton transfer. Interestingly, intense fluorescence, large Stokes-shift, and photostability are the various unique features of ESIPT-based probes (Fig. 7).
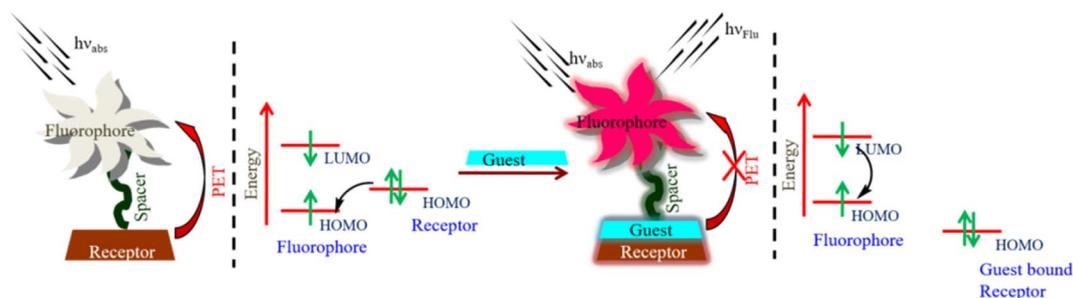

Fig. 4 Schematic representation of the photo-induced electron transfer (PET)-based sensing mechanism in ratiometric design.
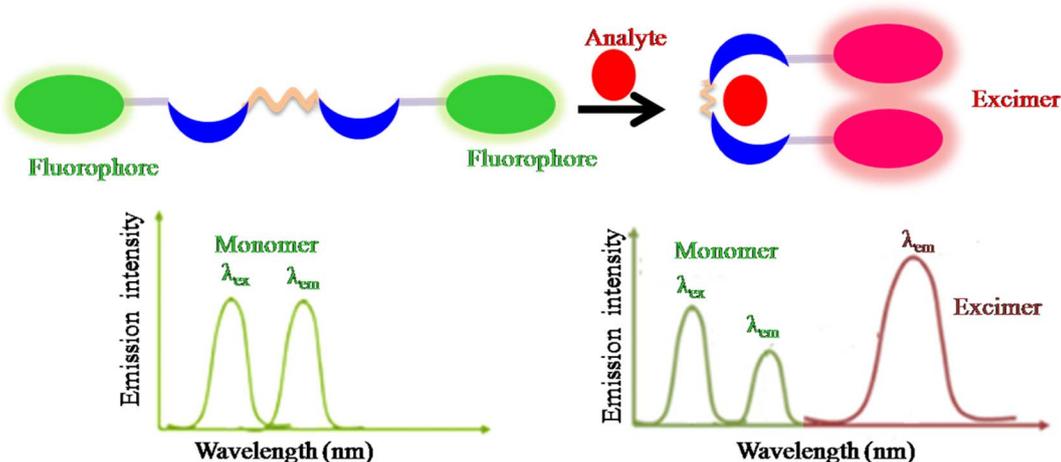

Fig. 5 Schematic representation of the monomer–excimer formation-based sensing mechanism in ratiometric design.
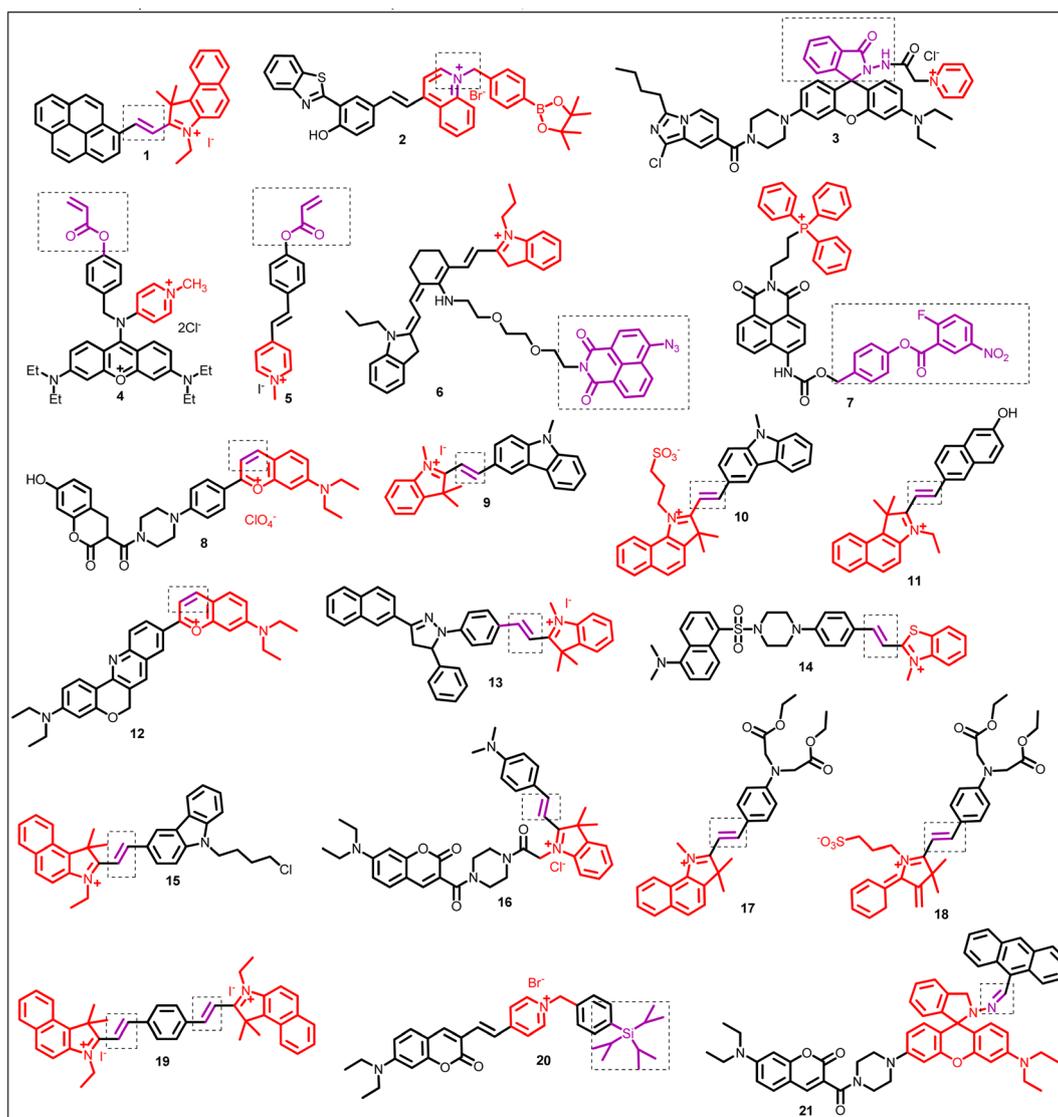
Fig. 6 Schematic representation of the Förster resonance energy transfer (FRET)-based sensing mechanism in ratiometric design.

Fig. 7 Schematic representation of the excited state intra-molecular proton transfer (ESIPT)-based sensing mechanism in ratiometric design.

4 Mitochondria-targeting ratiometric fluorescent probes

Mitochondria are organelles that play a vital role in cell physiology, including oxidative respiration, ATP production, and signal transduction. Mitochondria are widely known as the main generators of various ROS, RSS and RNS. Thus, probes that can specifically target mitochondria play a key role in monitoring multiple functions of mitochondria and mitochondrion-related illnesses.[59–62]

4.1 Reactive oxygen species (ROS) detection in mitochondria

The reactive oxygen species H_2O_2 and HOCl are potent oxidants with antibacterial capabilities.[63,64] However, the aberrant synthesis of ROS species *in vivo* has been linked to several illnesses, including lung damage, atherosclerosis, osteoarthritis, and rheumatoid arthritis.[27] Therefore, real-time and on-site detection of ROS is an exciting research topic.

Hu *et al.* constructed probe **1** with far-red emission by combining a pyrene unit (electron donor, high quantum yield, ability to form a complex in the excited state) with a benzo[*e*] indolium unit (electron acceptor, extended π-conjugation, mitochondrion-targeting group) linked by an ethylene bridge (Fig. 8, Table 1).[65] In EtOH/PBS solution, the free probe exhibited emission at 632 nm (λ_{ex} = 525 nm). Upon the addition

of ClO⁻, emission at 632 nm gradually fades away with a concomitant increase in fluorescence intensity at 455 nm (blue emission). Probe **1** with excellent mitochondrial targeting features, such as high selectivity (detection limit = 182 nM), fast response time, significant Stokes–Stokes shift (107 nm), photostability, and live cell membrane permeability, displayed potential for detecting ClO⁻ in mitochondria.

An important ROS, endogenous H_2O_2, functions as a signaling molecule to control various cellular processes, such as cell division, proliferation, and migration.[66,67] However, high H_2O_2 concentrations can harm proteins and nucleic acids, which are strongly related to many disorders such as malignancies, diabetes, and Alzheimer's disease.[68,69] Therefore, monitoring of H_2O_2 concentration is essential. He *et al.* designed benzothiazole dye (adequate stability, large Stokes-shift, large quantum yield, tunable emission) based probe **2** containing an aromatic boronic ester moiety (H_2O_2 recognition group) (Fig. 8, Table 1).[70] The fluorescence titration of probe **2** with H_2O_2 revealed an increase in new emission maxima at 594 nm at the expense of emission at 666 nm. The limit of detection was 23.1 nM. The sensing mechanism was the H_2O_2 triggered aromatic boronic ester moiety removal. Furthermore, probe **2**, with excellent mitochondrial targeting properties, such as significant Stokes shift (152 nm), photostability, and Pearson's colonization coefficient (0.94), displayed potential for detecting H_2O_2 in mitochondria.

Shen *et al.* designed probe **3** based on the FRET platform for detecting OCl⁻ (Fig. 8, Table 1).[71] In the presence of OCl⁻, probe **3** displayed ratiometric fluorescence change, and the plot of intensity ratio (I_{575}/I_{467}) with the concentration of OCl⁻ was linear in the range of 0 to 5 μM. The limit of detection was 10.2 nM. From the fluorescence imaging experiment, the applied probe **3** successfully examined endogenous OCl⁻ in Murine RAW 264.7 cells.

4.2 Reactive sulfur species (RSS) detection in mitochondria

Reactive sulfur species (RSS), such as cysteine (Cys), hydrogen sulfide (H_2S), and hydrogen polysulfides (H_2S_n), are produced in large quantities in mitochondria and are associated with critical mitochondrial-related pathological and physiological processes.[7] Cys can act as an antioxidant in mitochondria by removing various ROS from mitochondria to stop oxidative damage.[72] Additionally, Cys is necessary for the mitochondrial

Fig. 8 Chemical structure of mitochondrion-targeting ratiometric fluorescent probes (**1–21**) (red color: mitochondrion-targeting unit; purple color with dotted box: response site).

process of protein turnover.[73–75] Therefore, it is essential to identify and measure Cys in real-time within cells, particularly in the mitochondria, to understand the pathological and physiological processes properly.

Yang *et al.* designed xanthylene-based fluorescent probe **4** for the ratiometric detection of cysteine levels in the mitochondria (Fig. 8, Table 1).[21] The probe **4** containing an acryloyl moiety (responsive site for cysteine) and a benzyl group (for easy distribution in the mitochondria) showed strong red fluorescence at λ_{em} = 605 nm (λ_{ex} = 490 nm). In the presence of cysteine, probe **4** underwent ratiometric fluorescence change with the formation of new emission maxima at 540 nm and the simultaneous decrease in emission intensity at 605 nm. The limit of detection was 33.7 nM for cysteine. Applied probe **4** examined endogenous cysteine levels in HeLa cells through bioimaging, demonstrating potential applications in natural areas.

Considering the advantage of two-photon fluorescence microscopy and ratiometric detection, Niu *et al.* developed probe **5** for detecting cysteine over other biothiols (Fig. 8, Table 1).[76] In the presence of cysteine, the fluorescence spectrum of probe **5** exhibited ratiometric change (I_{518}/I_{452}), linear in the range between 0.5 and 40 µM. Interestingly, the merocyanine fluorophore and probe **5** exhibited a large two-photon cross-section ($\Phi_{\sigma_{max}}$) of 72.6 GM (λ_{ex} = 760 nm) and 65.2 GM (λ_{ex} = 740 nm), respectively, favorable in producing bright and high contrast images of living samples. In addition to detecting cysteine in live cells and mitochondria, probe **5** exhibited promising application for monitoring cysteine concentration in living tissues (down to 150 µm depth) using two-photon fluorescence microscopy.

H$_2$S plays essential roles in mitochondria, such as scavengers for reactive oxygen species,[77] and is associated with various mitochondrial-related pathological and physiological

Table 1 Summary of organelle-targeting ratiometric fluorescent probes

BS	Organelle	Targeting moiety	Analyte	Λ_{ex} (nm)	Λ_{em} (nm)	Stokes shift (nm)	LOD	Sensing mechanism	Application	Ref.
1	Mitochondria	Benzo[e]indolium group	ClO^-	525	I_{632}/I_{455}	107	182 nM	Reaction based and ICT process	HOCl investigation in biological samples	65
2	Mitochondria	Positively charged probe	H_2O_2	440	I_{594}/I_{666}	102–254	23.1 nM	ICT and ESIPT mechanisms	H_2O_2 detection in living HeLa cells	70
3	Mitochondria	Quaternized pyridine moiety	ClO^-	370	I_{575}/I_{467}	—	10.2 nM	FRET process	Mitochondrial OCl^- related studies	71
4	Mitochondria	Positively charged fluorophore	Cysteine	514	I_{540}/I_{605}	90	33.7 nM	Reaction-based	Quantitatively tracking the Cys distributions in mitochondria	21
5	Mitochondria	Positively charged fluorophore	Cysteine	350	I_{518}/I_{452}	—	—	Reaction based	Monitoring cysteine level in live cells and in living tissue	76
6	Mitochondria	Cationic cyanine moiety	H_2S	428 and 636	I_{530}/I_{733}	—	1.31 μM	ICT process and reaction based mechanism	Monitoring mitochondrial H_2S in living cells	24
7	Mitochondria	Triphenylphosphonium group	H_2S_n	405	I_{550}/I_{485}	109	20 nM	Reaction based	To study H_2S-linked physiological and pathological processes	81
8	Mitochondria	Benzopyrylium structure	SO_3^{2-}	405	I_{455}/I_{635}	230	0.078 μM	Nucleophilic addition reaction and FRET process	SO_3^{2-} imaging in biological systems	88
9	Mitochondria	Indolium group	HSO_3^-	350	I_{490}/I_{590}	—	0.15 μM	Nucleophilic addition reaction	Monitoring SO_2 derivatives in living cells	89
10	Mitochondria	Benzoindole group	SO_2 derivatives	405	I_{463}/I_{625}	—	58 nM	Nucleophilic addition reaction	Monitoring SO_2 derivatives in living cells	90
11	Mitochondria	Cyanine dyes	SO_3^{2-}/HSO_3^-	404	I_{467}/I_{593}	—	3.6 nM	1,4-Addition reaction	Monitoring SO_2 derivatives in living cells	91
12	Mitochondria	Positively charged fluorophore	$NaHSO_3$	405 and 580	I_{514}/I_{613}	—	103 nM (λ_{ex} = 580 nm) and 17 nM (λ_{ex} = 405 nm), separately	Nucleophilic addition reaction and ICT process	Detection of SO_2 derivatives in mitochondria under one-photon and two-photo absorption	92
13	Mitochondria	Hemi-cyanine dyes	SO_2 derivatives	380 and 558	I_{480}/I_{640}	—	80 nM	Nucleophilic addition reaction and ICT process	Detection of SO_2 derivatives in mitochondria	93
14	Mitochondria	Benzothiazolium moiety	Bisulfite	390	I_{540}/I_{590}	—	69 nM	Nucleophilic addition reaction and FRET process	Quantitative detection of HSO_3^- in mitochondria	94

Table 1 (Contd.)

BS	Organelle	Targeting moiety	Analyte	λ_{ex} (nm)	λ_{em} (nm)	Stokes shift (nm)	LOD	Sensing mechanism	Application	Ref.
15	Mitochondria	Lipophilic cationic dye probe	HSO_3^-	322 and 510	I_{462}/I_{588}	—	10 nM	1,4-Nucleophilic addition reaction	Detection of SO_2 derivatives in living cells	95
16	Mitochondria	Indole moiety	SO_3^{2-}	430	I_{476}/I_{589}	—	12.85 nM	Nucleophilic addition reaction, ICT process and FRET effect	SO_3^{2-} imaging in living cells	96
17 and 18	Mitochondria	Cyanine dye, 1H-benzo[e]indolium	HSO_3^-/SO_3^{2-}	840	I_{476}/I_{579} and I_{468}/I_{586} for probes 17 and 18, respectively	169 and 166 for probes 17 and 18, respectively	0.20 μM and 0.11 μM for probes 17 and 18, respectively	Nucleophilic addition mechanisms, ICT process	SO_3^{2-} imaging in living cells	97
19	Mitochondria	Benz[e]indole moiety	HSO_3^-/SO_3^{2-}	380	I_{480}/I_{600}	—	0.1 μM	Nucleophilic addition mechanisms, ICT process	SO_3^{2-} imaging in living cells	98
20	Mitochondria	Pyridinium salt	F^-	490	I_{539}/I_{639}	—	12 nM	Si–O bond cleavage and ICT process	F^- investigation in biological samples	100
21	Mitochondria	Rhodamine dyes as fluorescent lipophilic cations	Pd^{2+}	400 and 550	I_{594}/I_{472}	—	—	Chelation induced ring opening of rhodamine spirolactam and FRET process	Ratiometric visualization of Pd^{2+} in mitochondria	29
22	Lysosome	Pyridine group	H_2O_2	375	I_{550}/I_{425}	125	12.8 nM	ICT process	Lysosomal H_2O_2 detection	37
23	Lysosome	Morpholine group	HOCl	370	I_{589}/I_{462}	—	10.2 nM	PET process, TBET process and HOCl induced ring opening of rhodamine spirocyclic form	To monitor HOCl changes in lysosome	15
24	Lysosome	Monothio-bishydrazide moiety	HOCl	410	I_{580}/I_{480}	—	0.66 μM	FRET process	HOCl detection in living cells	14
25	Lysosome	Morpholine	HOCl	440	I_{610}/I_{535}	—	0.58 μM	ICT process	Lysosomal HOCl detection in living cells and zebrafish	109
26	Lysosome	Morpholine moiety	Bisulfite	480	I_{512}/I_{704}	—	0.09 μM	1,6-Conjugate addition reaction	Ratiometric fluorescence imaging of lysosomal bisulfite	114
27	Lysosome	Morpholine moiety	Cysteine	510	I_{510}/I_{685}	—	0.28 μM	1,6-Conjugate addition	Fluorescence imaging of the lysosomal cysteine	117
28	Lysosome	Morpholine	H_2S	350	I_{415}/I_{560}	—	0.43 μM	FRET-based	H_2S detection in lysosome	118

Table 1 (Contd.)

BS	Organelle	Targeting moiety	Analyte	λ_{ex} (nm)	λ_{em} (nm)	Stokes shift (nm)	LOD	Sensing mechanism	Application	Ref.
29	Lysosome	Morpholine	Cu^{2+}	440	I_{580}/I_{519}		1.45 nM	FRET process	Lysosomal Cu^{2+} detection in living cells	123
30	Lysosome	Morpholine	Cu^{2+}	360 nm	I_{552}/I_{486}		105 nM	FRET process	Lysosomal Cu^{2+} detection in living cells	125
31	Lysosome	Morpholine	Hg^{2+}	480 nm	535 to 595 nm		0.23 µM	PET process	Lysosomal Hg^{2+} detection in living cells	127
32	ER	—	H_2O_2	395	I_{540}/I_{465}	—	38 nM	Reaction based mechanism	H_2O_2 detection in ER	131
33	ER	Methyl sulfonamide	HClO	For $\lambda_{em} = 554$, $\lambda_{ex} = 425$; for $\lambda_{em} = 588$, $\lambda_{ex} = 500$	I_{480}/I_{554}	—	0.59 µM	Reaction-based	HClO detection in the ER of living cells	39
the	ER	p-Toluenesulfonamide group	HClO	380	I_{484}/I_{533}		0.1 µM	ICT process and reaction-based	HClO detection in the ER of living cells	41
35	ER	—	HOCl	326	I_{450}/I_{361}	—	3.6 µM	Nucleophilic borono-Dakin oxidation mechanism	Study of ER signaling and function under oxidative stress	18
36	ER	—	H_2S	480	I_{650}/I_{560}	(~150 nm)	39.1 nM	Reaction based mechanism	H_2S detection in living cells and zebrafish	144
37	ER	—	SO_2 derivatives	440	I_{534}/I_{610}		16.2 nM	FRET process	Fluorescence imaging of HSO_3^-/SO_3^{2-} in living cells	147
38	ER	—	Cu^{2+}	410	I_{545}/I_{480}		1.1 µM and 0.7 µM for Cu^{2+} and Cu^+, respectively	Copper-promoted hydrolysis	Imaging copper accumulation in the ER of live cells	150
39	ER	p-Toluenesulfonamide	pH	405	I_{446}/I_{527}		Response to pH in the range 5.0–7.2	ICT–PET–FRET mechanism	Quantitative measurement of pH values in endoplasmic reticulum (ER)	40
40	ER	p-Toluenesulfonamide	Carboxylesterase 2 detection	380	I_{560}/I_{414}	—	—	Reaction-based	Carboxylesterase 2 detection in drug-induced acute liver injury	158
41	Golgi apparatus	Phenylsulfonamide group	H_2O_2	—	I_{560}/I_{470}	—	0.20 µM	Reaction-based	To monitor Golgi oxidative stress and novel drug targets	162
42	Golgi apparatus	Sulfanilamide	$ONOO^-$	—	I_{650}/I_{477}	—	—	Reaction-based	To monitor Golgi oxidative stress and to evaluate drug-induced liver injury	163

Table 1 (Contd.)

BS	Organelle	Targeting moiety	Analyte	λ_{ex} (nm)	λ_{em} (nm)	Stokes shift (nm)	LOD	Sensing mechanism	Application	Ref.
43	Golgi apparatus	Aminoquinoline derivative	CO	360	I_{520}/I_{425}	—	41 nM	Pd^0-mediated Tsuji–Trost reaction	Fluorescence imaging of CO in cells and zebrafish	164
44	Golgi apparatus	4-CF$_3$-7-aminoquinoline	Glutathione (GSH)	320	I_{510}/I_{425}	—	0.49 µM	Reaction-based	GSH detection and organelle-targeted therapy	165
45	Nucleolus	—	SO$_2$ and formaldehyde	365	I_{550}/I_{635}	—	0.17 µM	FRET process and Michael addition reaction	Living mice imaging 52	
46	Nucleus	—	NO	370	I_{530}/I_{424}	—	20 nM	Reaction based	Excellent candidate for use as a green fluorescent nucleus probe or a nucleic acid permanent stain	168
47	Nucleus	N-Methyl benzothiazole cations	Nucleus viscosity and G-QDNA	340	I_{650}/I_{407}	—	—	Twisted internal charge transfer (TICT)	Living cells	169
48	Lipid droplets and nucleus	Coumarin unit for lipid droplet and quinolinium unit for nucleic acid	Polarity change in the cellular environment	405	I_{470}/I_{670}	—	—	ICT process	Study of ferroptosis and ferroptosis-linked diseases through fluorescence imaging	170
49	Nucleus	Hoechst unit	DNA	345 nm	I_{505}/I_{450}	—	72 nM	FRET process	Excellent probe for the monitoring of nucleus DNA damage	171
50 and 51	Cytomembrane	Alkyl side chain of the pyridine salt	SO$_2$	415	I_{644}/I_{486}	—	—	Michael addition	Bio-application in a mice model	178
52	Plasma membrane	CAZ	pH	380 (basic form) and 480 (acidic form)	496 (basic form) and 566 (acidic form)	—	—	—	Imaging and measuring vesicular acidification	182
53	Mitochondria and lysosome	Semi-cyanine unit for targeting mitochondria and morpholine group for targeting lysosome	SO$_2$	400	I_{530}/I_{600}	—	0.82 µM	FRET process	Simultaneous detection of endogenous SO$_2$ in lysosome and mitochondria by one and two-photon modes.	183
54	Mitochondria and lipid droplets (LDs)	Hemi-cyanine to target mitochondria and neutral form of probe 54 to target LDs	pH	380	I_{450}/I_{580}	—	—	Reaction-based and ICT process	Furthermore, probe 54 was successfully applied for monitoring the pH fluctuation in living cells under different exotic chemicals	19

processes.[78,79] Therefore, monitoring of H_2S level in mitochondria is crucial. Liu *et al.* proposed probe **6** integrated with cyanine (mitochondria-targeting group) and naphthalimide group (responsive to H_2S) for ratiometric detection of H_2S in mitochondria (Fig. 8, Table 1).[24] In the CTAB solution, upon the addition of Na_2S, probe **6** displayed ratiometric fluorescence response, and the intensity ratio (I_{530}/I_{733}) showed good linearity in the range of 1–9 μM. The detection limit was 1.31 μM for Na_2S. In the presence of Na_2S, reduction of the azide group to the amino group (electron donating) occurs, activating the ICT process and turn-on fluorescence of the naphthalimide moiety. Probe **6** found applications for fluorescence imaging and ratiometric detection of H_2S in live cells.

Han *et al.* engineered probe **7** integrated with triphenylphosphonium (mitochondria-targeting group), 2-fluoro-5-nitrobenzoic unit, and 1,8-naphthalimide fluorophore (well-known ICT fluorophore)[80] for the detection of H_2S_n (Fig. 8, Table 1).[81] In the phosphate-buffered saline (PBS) solution, fluorescence titration of probe **7** with Na_2S_2 revealed a decrease in emission intensity at 485 nm. A new emission maximum at 550 nm emerged and increased (Stokes-shift = 109 nm). Probe **7** successfully demonstrated its application in imaging intracellular H_2S_n with good selectivity and sensitivity.

SO_2 is an essential endogenous signaling molecule that performs significant roles in many physiological processes. However, increased SO_2 concentration is associated with severe lung cancer, nervous system diseases, and respiratory problems.[82–85] Therefore, detecting SO_2 and its derivatives in living systems becomes a high priority. Notably, a platform with fluorophores attached to aromatic heterocycles through C–C bonds was frequently used as a Michael addition receptor. The Michael-addition principle allows nucleophiles, such as bisulfite, to attack the C–C double bond.[86,87] In this section, most probes for bisulfite detection follow the nucleophilic addition reaction mechanism.

Taking advantage of the merits of FRET-based systems such as a large Stokes-shift, Huang *et al.* developed near-infrared (NIR) fluorescent probe **8** by combining a coumarin carboxylic acid group with a piperazine substituted benzopyrylium salt (mitochondrion-targeting group) (Fig. 8, Table 1).[88] In PBS solution, the fluorescence spectrum of probe **8** exhibited emission maxima at 635 nm and a large Stokes-shift (230 nm). The nucleophilic addition reaction of SO_3^{2-} at the double bond of the benzopyrylium unit resulted in the interruption of the conjugated π-electron cloud, and the

fluorescence at 635 nm decreased, accompanied by the simultaneous increase in the new emission peak at 455 nm. From the co-localization experiment, probe **8** efficiently targeted mitochondria (Pearson's co-localization coefficient = 0.84), and further investigations in HeLa cells and the nude mice experiment showed the application of probe **8** in biological systems for detecting SO_3^{2-} (Fig. 9).

Liu *et al.* exploited probe **9**, prepared by the condensation reaction between indolium or pyridinium and 3-formyl-9-methyl carbazole unit (Fig. 8).[89] In the presence of HSO_3^-, probe **9** displayed ratiometric fluorescence change and the ratio of emission intensity (I_{490}/I_{590}) varied from 0.0383 to 3.8769 (101-fold enhancement). The *in vitro* imaging experiment proved the application of probe **9** for the quantification of SO_2 derivatives in the mitochondria.

The same group presented another probe, probe **10**, containing a carbazole and an alkyl sulfonated benzoindole (water soluble, mitochondria-targeting group) as the basic skeleton (Fig. 8, Table 1).[90] In the presence of HSO_3^-, the emission spectrum of probe **10** revealed a blue shift of 162 nm, and the emission intensity ratio (I_{463}/I_{625}) was 56 (Fig. 10). The change in proton signals from 8.03–8.78 to 5.15 after the addition of HSO_3^- in the ^1H NMR spectrum, together with NOESY and COSY results, proved a 1,4-addition reaction-based detection mechanism. Unlike other reported probes for mitochondrial SO_2 detection, probe **10** could monitor the mitochondrial SO_2 level variation stimulated by carbonyl cyanide *m*-chlorophenyl hydrazone (CCCP) or by drugs.

Based on the 1,4-addition reaction between the polymethine chain of hemicyanine and SO_3^{2-} or HSO_3^-, Wang *et al.* developed probe **11** to detect SO_2 derivatives in aqueous medium and the mitochondria of living cells (Fig. 8, Table 1).[91] Upon the addition of HSO_3^-, the fluorescence spectrum of probe **11** showed ratiometric fluorescence change and the plot of their ratio (I_{467}/I_{593}) *vs.* the concentration of HSO_3^- was linear in the range of 1–9 μM. The sensing mechanism could be attributed to the interruption of the π-conjugation of probe **11** upon the addition of HSO_3^- at the responsive site of probe **11**, leading to a ratiometric change in the absorption and fluorescence spectrum. The fluorescence co-localization experiment revealed the unique distribution of probe **11** within the mitochondria of live MCF-cells (Pearson's correlation coefficients = 0.931, and Mander's overlap = 0.872). Furthermore, the applied probe **11** examined mitochondrial SO_2 derivatives quantitatively through a fluorescence imaging experiment.
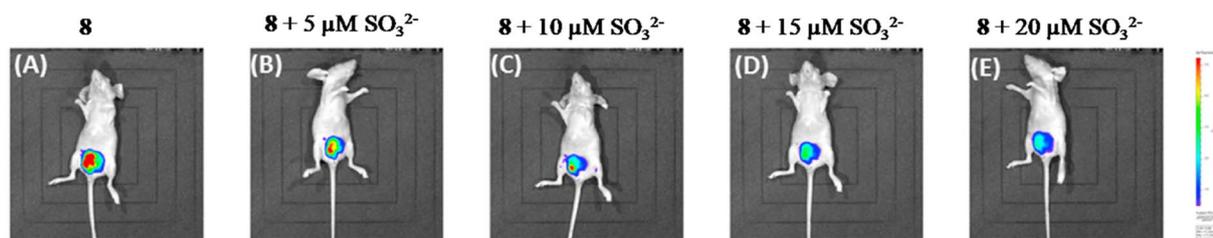

Fig. 9 *In vivo* photos of nude mice (A) 8 (20 μM); (B–E) 8 (20 μM) + different concentrations of SO_3^{2-} (5–20 μM). λ_{ex} = 530 nm, λ_{em} = 600–700 nm. Reprinted from ref. 88, copyright 2021 Elsevier.
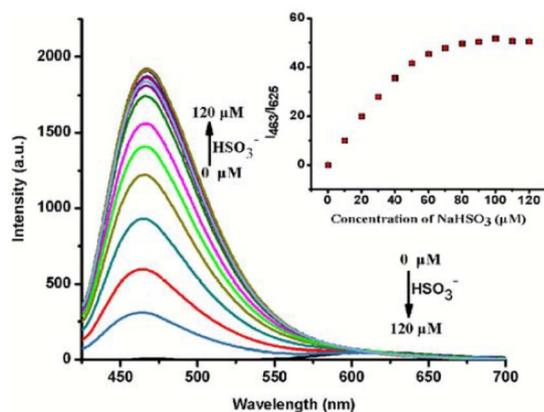
Fig. 10 Fluorescence titration spectrum of probe **10** with HSO_3^-. Inset: plot of intensity ratio (I_{463}/I_{625}) vs. [HSO_3^-]. Reprinted from ref. 90, copyright 2016 Royal Society of Chemistry.

Wang et al. applied the strategy of combining two classical dyes to construct long-wavelength probe **12**, prepared from benzopyrylium and chromenoquinoline dyes (Fig. 8, Table 1).[92] The emission spectrum of the two-photon fluorescent probe showed a gradual decrease in red fluorescence at 613 nm ($\lambda_{ex} = 580$ nm) and an increase in blue fluorescence at 514 nm ($\lambda_{ex} = 405$ nm) upon the addition of HSO_3^-. The detection limit was 103 nM and 17 nM for the red and green channels, respectively. The nucleophilic addition reaction of HSO_3^- at the C=C bond of probe **12** resulted in the interruption of π-conjugation/inhibition of the ICT process from the chromenoquinoline to the benzopyrylium group. Thus, a significant blue shift (99 nm) in the emission spectrum was observed. Furthermore, probe **12**

displayed application for detecting SO_2 derivatives in the solid state.

Wang et al. developed probe **13** based on pyrazoline (high quantum yield, cell permeability, and low cytotoxicity) and hemicyanine dyes (water soluble, mitochondrion-targeting group) (Fig. 8, Table 1).[93] The fluorescence titration of probe **13** with SO_3^{2-} revealed ratiometric fluorescence change, and the intensity ratio (I_{480}/I_{640}) changed from 0.45 to 445 (989 times). Intriguingly, probe **13** demonstrated an application for the ratiometric imaging of mitochondrial SO_2 derivatives in living cells.

Keeping in mind Michael's addition principle and the FRET process, Wu et al. designed probe **14** based on the conjugated platform of dansyl, piperazine, and benzothiazolium, in which the benzothiazole moiety acts as a recognition unit and mitochondrion-targeting group (Fig. 8, Table 1).[94] Upon the incremental addition of HSO_3^-, the fluorescence intensity ratio (I_{540}/I_{590}) of probe **14** showed a change from 0.3 to 1.5 (5-fold), and the limit of detection was 69 nM. Furthermore, probe **14** demonstrated a successful application for detecting HSO_3^- in the mitochondria of living cells through fluorescence imaging (Fig. 11).

α,β-Unsaturated compounds are prone to a nucleophilic addition reaction by HSO_3^-. With this in mind, Xu et al. prepared probe **15** by the condensation of 1H-benzo[e]indolium (water soluble, high quantum yield, significant Stokes shift (>100 nm), and mitochondrion-targeting group) with carbazole-3-aldehyde (Fig. 8, Table 1).[95] Upon the addition of HSO_3^-, the fluorescence spectrum of probe **15** underwent ratiometric fluorescence change with a decrease in the emission band at 588 nm and an increase in the new emission band at 462 nm, simultaneously. Interestingly, the cell staining experiment
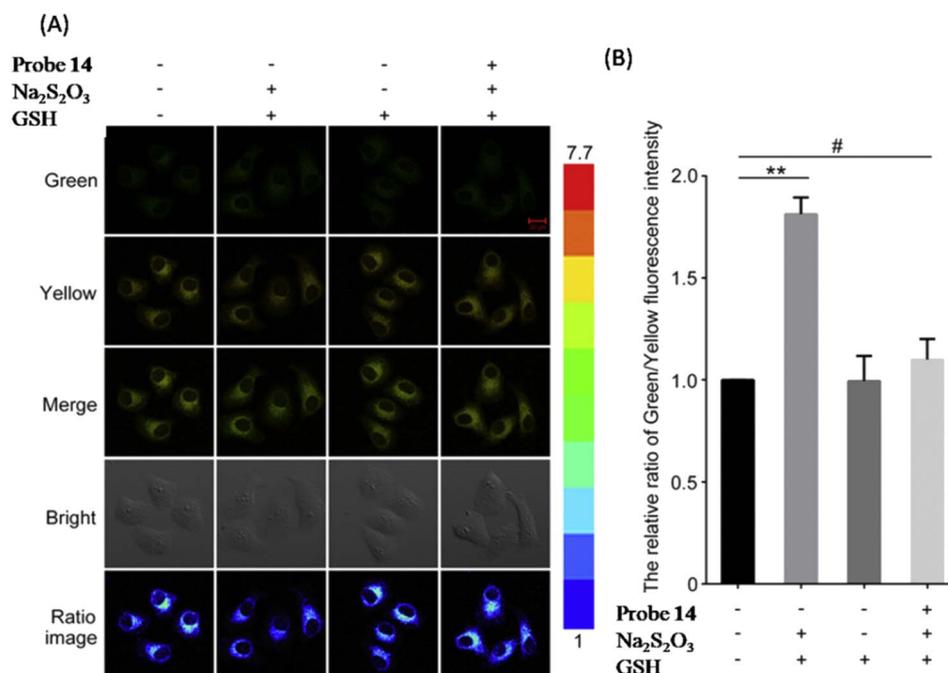
Fig. 11 (A) Confocal microscopic images of HepG2 cells demonstrating the application of probe **14** for HSO_3^- detection. (B) The relative intensity ratio (yellow/green) of columns 1, 2, 3 and 4 in (A). Reprinted from ref. 94, copyright 2017 Elsevier.

revealed probe **15** as cell-permeable and mitochondria-targetable, and it can monitor the intracellular SO_2 derivatives in live cells (HeLa cells).

Zhang *et al.* constructed probe **16** composed of the coumarin-hemicyanine skeleton, in which the FRET process occurs from coumarin to hemicyanine and the ICT process occurs from the styryl to the indolium group (mitochondrion-targeting) (Fig. 8, Table 1).[96] The nucleophilic approach of SO_3^{2-} towards the double bond of hemicyanine resulted in disruption of π-conjugation and interruption in the ICT/FRET process. This dual emission signal of probe **16** changed in a see-saw manner with a significant emission shift (113 nm). The staining experiment revealed probe **16** as a specific mitochondrion-targeting probe and can detect endogenous SO_3^{2-} in living cells such as HepG2 and L02 cells.

Zhao *et al.* developed probes **17** and **18** by using diethyl 2,2′-(phenylazanediyl)diacetate (electron-donor) and 1*H*-benzo[*e*] indolium (water soluble, high quantum yields, NIR emission property, and mitochondrion-targeting group) (Fig. 8, Table 1).[97] In the presence of HSO_3^-/SO_3^{2-}, probe **17** and **18** displayed ratiometric fluorescence change, blue-shift in emission (over 100 nm), and high selectivity and sensitivity (LOD = 0.20 μM and 0.11 μM for probes **17** and **18**, respectively). The sensing mechanism for both probes was a nucleophilic addition reaction. However, the path of the sensing mechanism was different. Interestingly, both the probes displayed the capability of quantifiable tracking and fluorescence imaging of HSO_3^-/SO_3^{2-} in the mitochondria of living cells.

Zheng *et al.* constructed probe **19** by the condensation reaction between trimethylbenzoindolium (mitochondrion-targeting moiety) and *p*-diphthalaldehyde (Fig. 8, Table 1).[98] The fluorescence response of probe **19** toward HSO_3^- was initially ratiometric (at low concentrations) and then turn-on emission (at high concentrations). The sensing mechanism was a twice nucleophilic addition reaction. The cell imaging revealed that the probe **19** could specifically detect HSO_3^- in the mitochondria of living cells (HepG2 cells).

4.3 Fluoride detection in mitochondria

The fluoride ion is one of the most significant anions crucial to many biological and medicinal processes. According to literature reports, a high fluoride ion concentration can damage mitochondria through oxidative stress and reduce the mitochondrial respiratory chain's efficiency, resulting in mitochondrial malfunction and the development of neurodegenerative disorders.[99] As a result, it is essential and beneficial to monitor fluoride ions in mitochondria.

Shen *et al.* applied ICT-modulated strategies for constructing probe **20** based on a diethylaminocoumarin derivative (a well-known ICT fluorophore) in which a pyridinium salt behaves as a mitochondrion-targeting group (Fig. 8, Table 1).[100] Initially, probe **20** exhibited red fluorescence at 639 nm (λ_{ex} = 490 nm) attributed to the ICT process between the pyridinium cation and 7-diethylamino-coumarin unit. Upon the addition of F^-, a new emission band at 539 nm emerged and increased at the expense of a decrease in emission at 639 nm. The sensing

mechanism was F^--induced cleavage of the Si–O bond between the phenyl and triisopropylsilyl groups. Furthermore, the applied probe **20** successfully examined mitochondrial F^- in living cells.

4.4 Palladium ion (Pd^{2+}) detection in mitochondria

Due to its high stability and reliability characteristics, palladium has been extensively employed in various applications, including catalysis, synthesis of organic compounds, medicine, dental crowns, fuel cells, and electronics production. However, palladium ion enrichment in living organisms can cause severe health-related diseases.[101,102] Therefore, developing an efficient tool for palladium ion detection in a biological system is necessary.

Wang *et al.* developed probe **21** to detect Pd^{2+} in living cells based on the FRET process and rhodamine ring-opening mechanisms (Fig. 8, Table 1).[29] In PBS buffer solution, free probe **21** exhibited emission maxima at 472 nm (λ_{ex} = 400 nm). Upon adding Pb^{2+}, a decrease in emission at 472 nm and an increase in the new emission band at 594 nm were observed. Moreover, the fluorescence imaging experiment revealed the application of probe **21** for the ratiometric visualization of Pd^{2+} in the mitochondria of living cells.

4.5 Challenges

Most organelle-targeting methods discussed above focus on lipophilic cationic fluorescent probes that selectively target mitochondria. However, problems with cationic probes, such as the effect on membrane potential and cellular toxicity, are yet to be overcome. Furthermore, to explain the probe's potential to target mitochondria, mostly co-localization experiments have been performed using commercially available mitochondria-specific dyes such as MitoTracker Green FM, MitoTracker Red, and MitoTracker Orange. However, there can be several other contributing factors and principles behind the probe's potential to target mitochondria, and these factors need a clear discussion.

In addition, mitochondria contain hundreds of biomolecules, such as anions, cations, enzymes, mitochondrial DNA, RNA, lipids, and so forth. Using fluorescent probes, it is still challenging to selectively label bioactive compounds at low concentrations (often nanomolar levels). No doubt, ratiometric fluorescent probes hold promise for removing various background interferences. However, nonetheless, just a few mitochondrion-targeting ratiometric fluorescent probes have been developed to date.

5 Lysosome-targeting ratiometric fluorescent probes

Lysosomes, an essential subcellular organelle, which can function as a digestive compartment in eukaryotic cells and include a variety of enzymes and proteins, are critical regulators in metabolic processes under acidic pH circumstances.[103] As key indicators of lysosome function and oxidative stress, reactive oxygen species (ROS) such as HClO and H_2O_2 and reactive

sulphur species (RSS) such as H_2S have been the focus of numerous probe designs. Since the lysosome lumen is acidic, developing probes that can detect HOCl in an acidic medium is challenging.[4,30]

5.1 Reactive oxygen species (ROS) detection in the lysosome

H_2O_2 is a significant reactive oxygen species (ROS) with distinct destructive oxidation characteristics. Lysosomes can produce hydrogen peroxide (H_2O_2) to combat pathogens.[104–106] Therefore, it's crucial to create a reliable method for measuring H_2O_2 in inflammatory tissues to assess the physiological and pathological link between lysosomal H_2O_2 and inflammation.

Inspired by the excellent optical properties of naphthalimide derivatives (donor–π-acceptor structured), Zhou et al. constructed probe 22 based on naphthalimide, benzylboric acid (H_2O_2 responsive group), and pyridine group (lysosome-targeting group) for monitoring H_2O_2 in living tissue and in inflamed tissue (Fig. 12, Table 1).[37] In the presence of H_2O_2, probe 22 displayed ratiometric fluorescence change, assigned to H_2O_2 mediated removal of the boric acid group from probe 22 and ICT effect. The fluorescence color of the solution changed from bright blue to light yellow. Furthermore, tissue imaging experiments using a confocal microscope demonstrated a potential application for H_2O_2 detection in inflamed tissues.

TBET-based probes offer several advantages, such as high energy transfer efficiencies, improved imaging resolution, and a large Stokes-shift.[107,108] With this in mind, Shen et al. synthesized probe 23 based on the imidazo[1,5-a]pyridine moiety (donor) and rhodamine moiety (acceptor) (Fig. 12, Table 1).[15] The free probe 23 exhibited emission at 462 nm attributed to the emission of the imidazo[1,5-a]pyridine fluorophore. Upon the gradual addition of aliquots of HOCl, the emission intensity at 462 nm almost remained constant, while a new emission maximum at 589 nm emerged and increased, assigned to the

rhodamine moiety. The sensing mechanism was the change of the rhodamine spiro form to the ring-open state in the presence of HOCl and the TBET process between the rhodamine unit and imidazo[1,5-a]pyridine. Applied probe 23 successfully monitored the HOCl changes in the lysosomes.

Using a similar mechanism to the one described above, which converts the rhodamine spiro-form into the ring-open form when HOCl is present, Yuan et al. provided the coumarin and rhodamine based FRET platform 24 for HOCl detection in living cells (Fig. 12, Table 1).[14] Upon excitation at 410 nm, probe 24 displayed emission at 480 nm (which belonged to the coumarin moiety). However, in the presence of HOCl, the emission spectrum of probe 24 showed a decrease in intensity at 480 nm and an increase in new maxima at 580 nm (which belonged to rhodamine), assigned to a ring-opening and FRET (FRET efficiency = 93.75%) based detecting mechanism.

Liu et al. constructed probe 25 from phenothiazine coumarin and a morpholine unit for hypochlorite detection (Fig. 12, Table 1).[109] The fluorescence titration of probe 25 with ClO^- showed a blue shift in emission from 610 to 535 nm. The sensing mechanism was inhibition of the ICT process due to the oxidation of the phenothiazine moiety. Furthermore, the fluorescence imaging experiment demonstrated the application of probe 25 for detecting ClO^- in living cells (RAW264.7 cells) and zebrafish (Fig. 13).

5.2 Reactive sulfur species (RSS) detection in lysosome

The endogenous oxidation of hydrogen sulfide or sulfur-containing amino acids produces bisulfite, which remains in equilibrium with sulfur dioxide and sulfite in aqueous media.[110–113] As a result, the discovery of bisulfite in lysosomes is of great interest.

Tamima et al. pioneered probe 26 by introducing a morpholine moiety (targeting group) to the benzopyronin dye
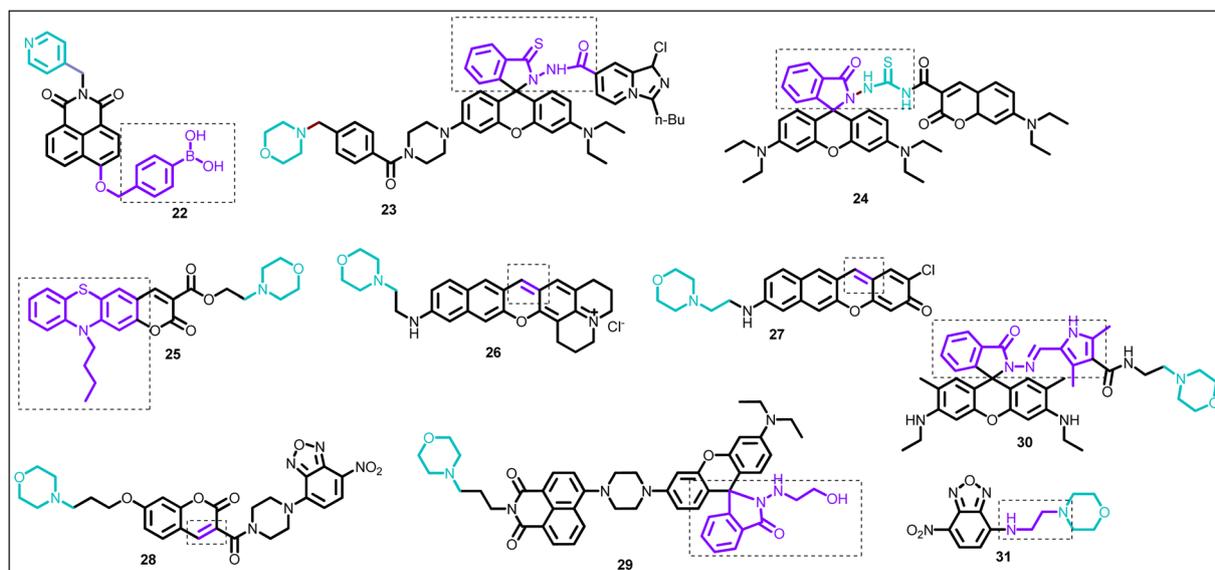

Fig. 12 Chemical structure of lysosome-targeting ratiometric fluorescent probes (22–31), (brown color: lysosome-targeting unit; purple color with dotted box: response site).
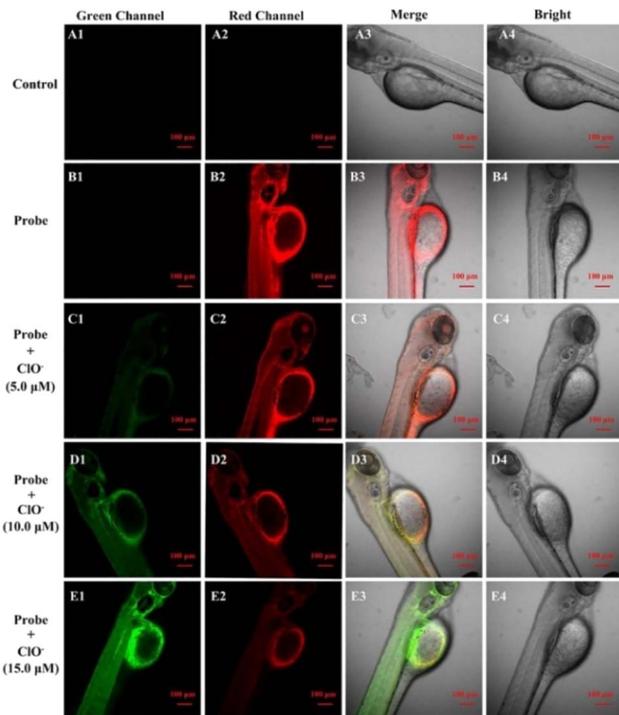
Fig. 13 Fluorescence images of zebrafish. The control group (A1–A4). Zebrafish co-cultured with probe **25** (10 μM) (B1–B4), followed by incubation with ClO⁻ 5 μM (C1–C4), 10 μM ClO⁻ (D1–D4) and 15 μM ClO⁻ (E1–E4). Reprinted from ref. 109, copyright 2021 Elsevier.

(Fig. 12, Table 1).[114] After adding bisulfite, the absorption and fluorescence spectrum of probe **26** displayed complete peak separation from 613 nm to 426 nm (spectral shift = 187 nm) and from 704 nm to 512 nm (spectral shift = 192 nm), respectively. The sensing mechanism was the 1,6-conjugate addition reaction. Probe **26** specifically targeted lysosomes and displayed application for monitoring intracellular bisulfite levels.

Cysteine, homocysteine, hydrogen sulfide, and glutathione are examples of cellular thiols frequently studied employing lysosome-targeting probes.[115] These biothiols are significant indications of lysosomal function because they are produced by lysosomal proteolysis.[116]

Tamima *et al.* devoted benzo[*b*]xanthene-derived probe **27** for the two-photon ratiometric fluorescence-based detection of cysteine (Fig. 12, Table 1).[117] The detecting mechanism of cysteine was a 1,6-conjugate addition reaction to the benzoxanthene core, resulting in the formation of a cysteine adduct that emitted red. However, in the presence of hydrogen peroxide, the 1-cysteine adduct was reverted to **27**. Furthermore, probe **27** demonstrated practical application to quantify cysteine levels in biological samples (human blood plasma).

Zhang *et al.* applied a cleavable FRET-based strategy for designing a lysosome-targeting probe **28**, based on a coumarin–NBD (nitrobenzofurazan) cassette (Fig. 12, Table 1).[118] Free probe **28** showed two emission maxima at 415 nm and 560 nm, belonging to the coumarin and NBD groups. Upon treatment with H₂S, probe **28** underwent ratiometric fluorescence change, the solution's emission color changed from yellow to blue, and

the intensity ratio increased from 0.22 to 67.7 (300-fold approx.). Furthermore, probe **28** preferentially targeted lysosomes and displayed potential application for detecting H₂S in lysosome.

5.3 Cu²⁺ detection in the lysosome

Many essential physiological processes involve the role of copper. Copper plays important roles in a variety of fundamental physiological processes.[119] At the organelle level, improper copper homeostasis can cause several severe illnesses.[120–122] As a result, it is still essential to monitor the concentration of copper levels in cells, particularly in lysosomes.

Liu *et al.* applied FRET-based strategies for constructing ratiometric probe **29** (Fig. 12, Table 1).[123] The probe **29** displayed high selectivity, sensitivity (detection limit = 1.45 nM), and ratiometric fluorescence response towards Cu²⁺. From fluorescence imaging experiments, live cells (L929 cells) incubated with probe **29** showed blue and weak green fluorescence. However, cells pre-treated with Cu²⁺ and then incubated with probe **29** showed solid green and diminished blue fluorescence. In addition, probe **29** was applied for fluorescence imaging of Cu²⁺ in the lysosome of living cells.

Inspired by Czarnik's report on Cu²⁺-induced ring opening of rhodamine,[124] Wu *et al.* synthesized probe **30** for Cu²⁺ detection (Fig. 12, Table 1).[125] In CH₃CN–H₂O (8 : 2) solution, probe **30** behaved as a selective and sensitive probe for Cu²⁺ over other tested ions. The sensing mechanism was Cu²⁺-induced ring opening and the FRET process from pyrrole to rhodamine.

5.4 Hg²⁺ detection in the lysosome

Mercury is a hazardous and pervasive heavy metal that can result in numerous serious health issues, including renal failure, damage to the central nervous system, *etc.*[126] Therefore, it is crucial to have an effective method for detecting mercury ions.

Zhang *et al.* developed an NBD-based probe **31** by introducing a morpholine moiety to the NBD fluorophore for Hg²⁺ detection (Fig. 12, Table 1).[127] In the presence of Hg²⁺, the absorption spectrum of probe **31** showed a red shift of the peak from 470 nm to 494 nm, and the color detected by the naked eye changed from light yellow to red. Under similar conditions, the fluorescence spectrum also revealed a red shift of emission maxima from 535 nm to 595 nm. Herein, the morpholine unit played dual roles as a ligand for Hg²⁺ and lysosome-targeting group. The sensing mechanism was assigned to the inhibition of the PET process from the nitrogen atom of morpholine to the NBD fluorophore upon coordination with Hg²⁺.

5.5 Challenges

Lysosome-based research has advanced significantly in recent years. Nevertheless, there are still several challenges for these probes. The synthetic probe cannot differentiate between autolysosomes, autophagosomes, endosomes, and other acidic compartments. These probes are harmful to live cells and inappropriate for long-term detection because they make lysosome alkaline. As a result, lysosome-specific probes devoid of

the alkalization effect are necessary. Most of the developed probes have emissions in the visible region, thus, cannot be used for deep-tissue imaging due to the poor penetration power.

6   Endoplasmic reticulum-targeting ratiometric fluorescent probes

The most prominent organelle in a cell, the endoplasmic reticulum (ER), is crucial for protein synthesis, folding, distribution, and calcium ion storage. Literature reports revealed that ER stress, which is linked to significant diseases, can cause autophagy and even cell death. Therefore, studying ER is an exciting field of research.[128,129]

6.1   Reactive oxygen species (ROS) detection in endoplasmic reticulum

H_2O_2, an important reactive oxygen species, plays a crucial role in various pathological and physiological processes. During ER stress, the increased concentration of H_2O_2 can damage cellular proteins and may result in cancer, metabolic diseases, cardiovascular diseases, neurodegenerative diseases, etc.[130,131] Therefore, developing efficient analytical methods for H_2O_2 in ER is crucial.

In the past, researchers developed various probes for detecting exogenous H_2O_2 in ER. However, quantitative detection of endogenous H_2O_2 remains challenging. To solve this issue, Gao et al. synthesized probe 32 based on α-ketoamide and naphthalimide groups (Fig. 14, Table 1).[131] Upon adding H_2O_2, the fluorescence spectrum of probe 32 revealed ratiometric fluorescence change, attributed to the reaction between H_2O_2 and α-ketoamide and subsequent hydrolysis of amido linkage. The limit of detection was 38 nM for H_2O_2. Furthermore, applied probe 32 found application for quantitative measurement of endogenous H_2O_2 in ER of living cells (HeLa cells), both

under normal conditions (0.692 μM H_2O_2) and under ER stress (1.26 μM H_2O_2).

In the past, the diaminomalenonitrile-based Schiff base has been used by several researchers for developing ClO$^-$ specific sensors.[132–134] On the other hand, the sulfonamide group has been known to target ER.[135] Taken together, Hou et al. constructed biosensor 33 for ClO$^-$ detection in ER (Fig. 14, Table 1).[39] Upon the addition of ClO$^-$, the fluorescence spectrum of biosensor 33 displayed a blue shift in emission wavelength from 554 nm to 480 nm, attributed to the reaction-based sensing mechanism. The plot of emission intensity ratio (I_{480}/I_{554}) vs. ClO$^-$ concentration was linear between 0 and 120 μM concentrations. The detection limit was 0.59 μM for ClO$^-$. The applied biosensor 33 examined exo/endogenous ClO$^-$ in the ER of living cells.

Inspired by the excellent optical properties and ICT process of 4-aminonaphthalimide moiety,[136] Ma et al. constructed biosensor 34 using a 4-aminonaphthalimide moiety (fluorescent group), (2-aminoethyl) thiourea unit (HClO recognition site), and p-toluenesulfonamide unit (ER-targeting group) (Fig. 14, Table 1).[41] In ethanol–H_2O (1 : 1, v/v) solution, free sensor 34 showed emission at 533 nm (green emission), attributed to the ICT process. After adding HOCl, biosensor 34 revealed ratiometric fluorescence change with blue-shift (49 nm) of the emission maxima from 533 nm to 484 nm, which was assigned to inhibition of the ICT process. Furthermore, biosensor 34 demonstrated an application for HOCl detection in the ER of PC-12 cells.

In the past, aryl boronic acid has been widely utilized in designing fluorescent sensors for biological species,[137] such as peroxynitrite (ONOO$^-$),[138] hypochlorite (OCl$^-$)[139] and hydrogen peroxide.[140,141] Pak et al. designed NHC-borane-based fluorescent sensor 35, constructed from a naphthoimidazolium precursor (HOCl responsive unit) for specific detection of HOCl
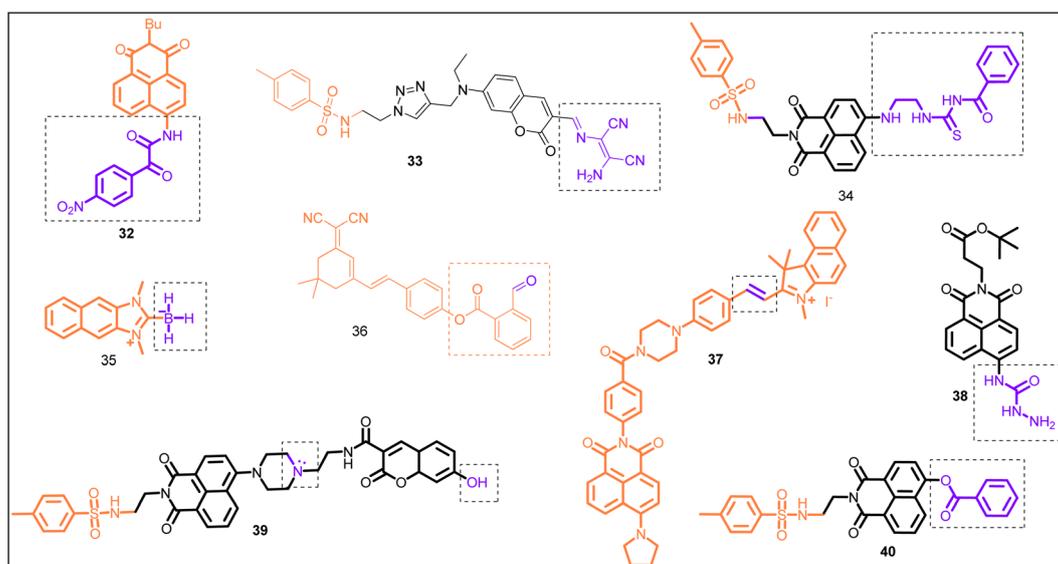

Fig. 14 Chemical structure of endoplasmic reticulum-targeting ratiometric fluorescent probe (32–40), (orange color: ER-targeting unit; purple color with dotted box: response site).

over other ROS (Fig. 14, Table 1).[18] Sensor **35** followed an electrophilic oxidation mechanism that involved B–H bond cleavage. Sensor **35** successfully targeted ER and demonstrated an application for monitoring HOCl in living cells (Raw 264.7 cells) and rat hippocampal slices by a two-photon fluorescence microscopy experiment.

6.2 Reactive sulfur species (RSS) detection in endoplasmic reticulum

Taking into account the essential role of H_2S during ER stress and ER functions,[142,143] Shu *et al.* pioneered ratiometric NIR-fluorescent biosensor **36** based on dicyano-isophorone (NIR emission, large Stokes-shift) and an *O*-carboxybenzaldehyde unit (H_2S recognition site) for H_2S detection in ER (Fig. 14, Table 1).[144] Sensor **36** showed fluorescence emission at 560 nm due to the ICT effect. Upon the gradual addition of H_2S, a new emission peak at 650 nm appeared and increased with the simultaneous decrease in λ_{em} at 560 nm. The sensing mechanism was a nucleophilic addition reaction. Furthermore, sensor **36** demonstrated an application for monitoring H_2S in living cells (HeLa cells) and zebrafish. Interestingly, sensor **36** successfully detected endogenous H_2S produced during ER stress incited by Tunicamycin.

Nowadays, physiological functions of SO_2 and its derivatives are gaining increasing attention. According to literature reports, SO_2 is vital in cardiovascular processes[145] and can regulate hippocampal neuron apoptosis.[146] Thus, SO_2 detection is essential. Li *et al.* developed a FRET-based platform **37**, constructed from benzoindole-based hemicyanine (acceptor) and naphthalimide derivatives (donor), for the detection of SO_2 derivatives in ER (Fig. 14, Table 1).[147] Sensor **37** exhibited emission maxima in buffer solution at 610 nm ($\lambda_{ex} = 440$ nm), attributed to the FRET process. The sensing mechanism was a nucleophilic addition reaction and inhibition of the FRET process. Furthermore, sensor **37** successfully targeted ER and demonstrated an application for imaging exogenous and endogenous SO_2 derivatives in living cells.

6.3 Cu^{2+} detection in endoplasmic reticulum

Mitochondria and lysosomes implicate the cellular homeostasis of copper.[148] Furthermore, lysosomes in damaged tissue contained high concentrations of copper ions.[149] However, it is unclear whether or not the copper ions in these organelles are the cause of the ER's harmful actions. Thus, to understand copper-related diseases, a reliable technique for imaging copper at the level of organelles is crucial.

Park *et al.* presented a naphthalimide and hydrazide based biosensor **38** for copper ion detection in living cells (Fig. 14, Table 1).[150] Upon the addition of copper ion to the solution of sensor **38** in HEPES buffer, the emission maxima were red-shifted (380 nm to 440 nm), and solution color changed from blue to yellowish-green. The detecting mechanism was assigned to the copper-mediated hydrolytic reaction of sensor **38**, forming aminonaphthalimide. Additionally, the biocompatible sensor **38** specifically targeted the ER of living cells and

displayed potential for qualitative and quantitative detection of Cu^+/Cu^{2+} under physiological conditions.

6.4 Monitoring pH in endoplasmic reticulum

The physiological functions of the ER, such as targeting during secretion, protein sorting, and retrieving resident chaperones, are regulated by the pH of the ER, which serves as a crucial parameter.[151] The ER pH is the same as that of the cytoplasm under normal physiological conditions.[152] Recent research has shown that ER stress potently stimulates autophagy, strongly linked to many diseases (such as cancer, infectious disorders, and neurodegeneration), causing the ER pH to drop.[153,154] Therefore, it is crucial to quantitatively evaluate the pH change in ER to explain the biological functions of ER fully.

Fluorescent probes with dual responsive sites have shown improved sensitivity to pH and enhanced emission wavelength.[155] With this in mind, Dong *et al.* pioneered probe **39** based on the naphthalimide–coumarin platform and employed hydroxyl and morpholine groups as the pH-responsive sites (Fig. 14, Table 1).[40] On excitation at 405 nm, the fluorescence spectrum of probe **39** showed ratiometric change with a single emission band at 527 nm (acidic pH, 4.09–5.08) and two emission maxima at 446 nm and 527 nm between pH 5.08 and 7.73, and further single emission maxima at 446 nm at pH 7.73 (basic pH). The sensing mechanism was assigned to the FRET–PET–ICT process (Fig. 15). Furthermore, due to the presence of the *p*-toluenesulfonamide group (ER-targeting group), probe **39** successfully targeted ER. It demonstrated an application for quantitatively detecting the pH changes in the dexamethanose-treated cell and during ER stress.

6.5 Carboxylesterase 2 (CES2) detection in endoplasmic reticulum

Carboxylesterase 2 (CES2) has critical roles in ER, such as metabolic, drug detoxification, molecular target for the prodrug design, and ER stress-associated diseases.[156,157] Tian *et al.* developed ratiometric fluorescent probe **40** based on *p*-toluenesulfonamide (ER-targeting group) for CES2 detection (Fig. 14, Table
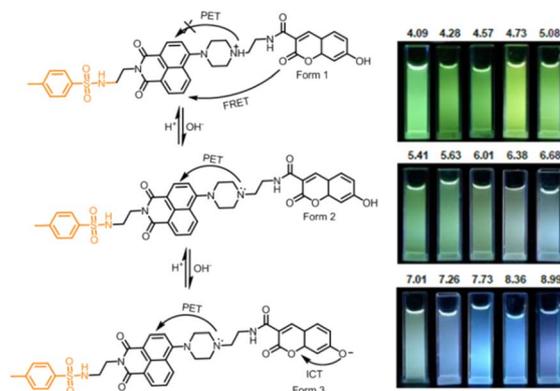

Fig. 15 (A) The sensing mechanism of probe **39** to pH. (B) Fluorescence images of probe **39** at different pH under illumination at 365 nm. Reprinted from ref. 40, copyright 2019 Royal Society of Chemistry.
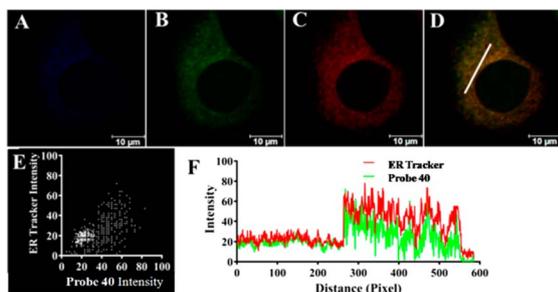
Fig. 16 Fluorescence images of probe **40** in HepG2 at the (A) blue channel (425–475 nm); (B) at the green channel (535–585 nm); (C) ER-Tracker (red); (D) merged image (green channel and ER-Tracker channel (red)); (E) intensity scatter plot; and (F) intensity plot for the region of interest (white line in panel D). Reprinted from ref. 158, copyright 2019 American Chemical Society.

1).[158] Among various hydrolases, only CES2 catalyzed the hydrolysis of probe **40**. Probe **40** was applied for imaging CES2 in living cells (HepG2 cells) and tumor tissue (Fig. 16). Notably, Probe **40** revealed a significant decrease in CES2 activity under ER stress and drug (acetaminophen (APAP))-induced liver injury model.

6.6 Challenges

Over the past few years, scientists engineered several ER-targeting fluorescent probes for the selective detection of various substances like NO, H_2S, H_2O_2, and HOCl. However, the mechanism behind ER selectivity still needs to be clarified. Many biological species present in ER still need to be detected due to a lack of efficient probes. In addition, most of the probes discussed above emit visible light. Thus, their *in vivo* applicability is restricted.

7   Golgi apparatus-targeting ratiometric fluorescent probes

The Golgi apparatus is an organelle with a phospholipid membrane composed of cisterna. It transforms proteins from the rough ER, then separates them into vesicles for transport to other cell regions. According to recent findings, CO is crucial for the Golgi apparatus.[159–161] Thus, to study in depth various functions of the Golgi apparatus, it is essential to develop efficient Golgi apparatus-targeting probes.
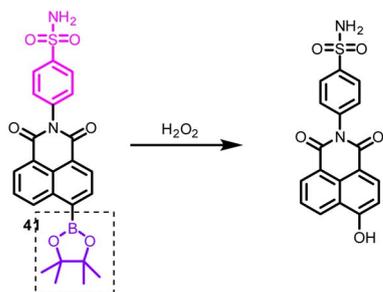

Fig. 17 Reaction-based detection mechanism of probe **41** for H_2O_2.

7.1   Reactive oxygen species (ROS) detection in Golgi apparatus

Golgi oxidative stress is closely linked to the occurrence and progression of hypertension, and the concentration of hydrogen peroxide (H_2O_2) plays a critical role in this process. To address this issue, Wang *et al.* developed a two-photon fluorescent probe **41**, which targets the Golgi apparatus with the aid of a phenylsulfonamide group. The response mechanism was a reaction-based process (Fig. 17).[162] Upon reacting with H_2O_2, the boric acid ester is transformed into a hydroxyl group that donates electrons, thereby promoting the push–pull electron effect of the naphthalimide-conjugated system. This leads to the production of strong fluorescence emission. The probe **41** enables *in situ* H_2O_2 ratiometric imaging in living systems and provides a highly effective means to monitor Golgi oxidative stress. The probe **41** was able to identify the generation of H_2O_2 during Golgi oxidative stress and demonstrated increased levels of Golgi H_2O_2 in the kidneys of hypertensive mice.

7.2   Reactive nitrogen species (RNS) detection in Golgi apparatus

The detection of peroxynitrite ($ONOO^-$) is essential for the study and treatment of drug-induced liver injury (DILI) associated with oxidative stress. Targeting the Golgi apparatus has emerged as a new approach for DILI research and treatment. Feng *et al.* developed a new probe, **42**, by conjugating a sulfanilamide moiety to a coumarin–hemi-cyanine conjugated system (Fig. 18).[163] The probe displayed high sensitivity, selectivity, and low cytotoxicity, and showed a rapid ratiometric fluorescence response to $ONOO^-$. Unexpectedly, probe **42** also displays unique targeting properties in living cells, with the ability to label the cell membrane first and then the Golgi. Imaging experiments with probe **42** showed it to be effective in monitoring $ONOO^-$ under Golgi oxidative stress and in DILI using mice models.

7.3   CO monitoring in Golgi apparatus

Inspired by the recent reports on the fluorescent probe for CO detection based on the Tsuji–Trost reaction and to understand in depth the role of CO in subcellular organelles, Zheng *et al.* constructed probe **43** (Fig. 19, Table 1). On excitation at 360 nm, probe **43** exhibited emission at 425 nm.[164] Upon the addition of CORM-3 (CO donor), probe **43** showed a significant 95 nm red shift with a decrease and increased emission maxima at 425 nm and 560 nm, respectively. The detecting mechanism was attributed to the cleavage of the allycarbamate group of probe
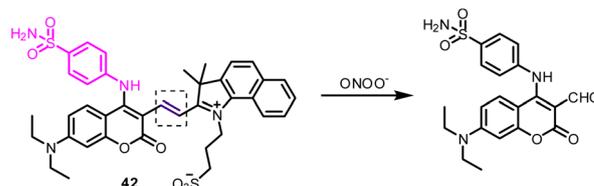

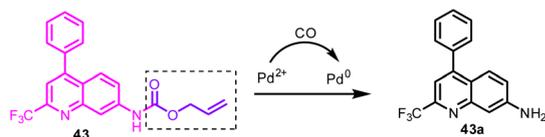**Fig. 18** Reaction-based detection mechanism of probe **42** for $ONOO^-$.

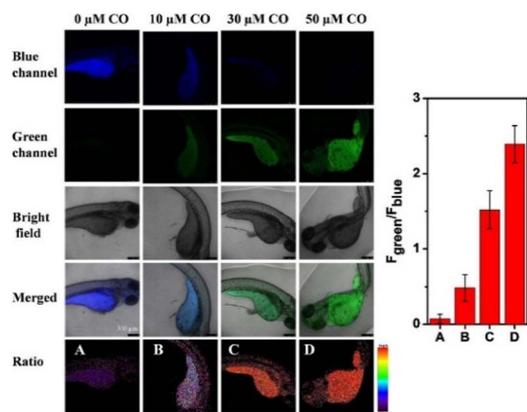**Fig. 19** Sensing mechanism of probe **43** for CO detection based on Tsuji–Trost reaction.

Fig. 20 CO fluorescence imaging in zebrafish with probe **43**. The right figure exhibits the fluorescence intensity ratio value (green/blue). Reprinted from ref. 164, copyright 2021 Elsevier.

43 to form **43a** mediated by a Pd^0 Tsuji–Trost reaction. Furthermore, probe **43** found application for CO imaging in cells and zebrafish and to visualize CO levels during cellular oxidative stress stimulated by lipopolysaccharide (Fig. 20).

7.4 Glutathione (GSH) detection in Golgi apparatus

The high expression of antioxidants like glutathione in cancer cells helps them withstand oxidative stress within the Golgi apparatus. Thus, monitoring changes in glutathione concentration within the Golgi could serve as an effective way to track the occurrence and progression of tumor cells. Rong *et al.* created a Golgi-targeting probe **44** that could detect GSH with high accuracy.[165] The fluorescence titration experiment of probe **44** with GSH revealed a decrease in intensity at 425 nm and emergence of a new peak at 510 nm. The detection limit was 0.49 μM for GSH. The response mechanism was a reaction-based process (Fig. 21). Furthermore, the Golgi stress response experiment revealed the ability of probe **44** for *in situ* endogenous GSH detection in the Golgi apparatus during oxidative stress.
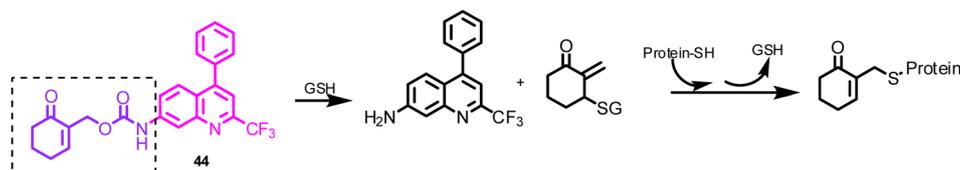
7.5 Challenges

The Golgi apparatus-targeting ratiometric fluorescent probes are rare in the literature. Furthermore, the targeting mechanism is not clear.

8 Nucleus-targeting ratiometric fluorescent probes

For both cancer treatment and genetic engineering, the cell nucleus has been a primary target since it stores the genetic material that is protected by the nuclear envelope, which is made up of two lipid bilayer membranes.[166]

8.1 Reactive sulphur species (RSS) detection in the nucleus

Organisms' excessive generation of formaldehyde (FA) and sulfur dioxide (SO$_2$) is directly linked to several ailments, such as genotoxicity, respiratory disease, and neurological abnormalities. However, the protective barrier of the cell nucleus membrane makes it challenging for fluorescent probes to investigate the correlation of FA and SO$_2$ in the nucleolus regions. Ma *et al.* took this challenge and constructed probe **45** based on the benzopyryllium-dansyl FRET platform (Fig. 23, Table 1).[52] The probe **45** was used for SO$_2$ reversible sensing and recovered by FA. The sensing mechanism of SO$_2$ was the interruption of the FRET process between dansyl (donor) and benzopyryllium (acceptor). The FA addition restored the FRET process because of the reversible Michael addition reaction. Probe **45** found application for quantitatively monitoring endogenous SO$_2$/FA in the nucleus region of live cells and living animals.

8.2 Reactive nitrogen species (RNS) detection in the nucleus

Nitric oxide (NO) is a significant signal molecule involved in a variety of physiological and pathological processes. Thus, to understand these processes, real-time detection of short-living NO in the biological medium is crucial. Based on their previous reports on NO detection,[167] Li *et al.* developed probe **46** for NO detection in living cells.[168] The fluorescence spectrum of probe **46** showed a ratiometric change in fluorescence with NO, and the plot of intensity ratio I$_{530}$/I$_{424}$ *vs.* NO concentration was linear between 0 and 40 μM. The sensing mechanism was a reaction-based process in which **46m** reacted with NO to generate product **46p** (Fig. 22, Table 1). In living RAW 264.7 cells, **46m** can detect both exogenous and endogenous NO. It's interesting to note that **46m** and its sensing product **46p** both show localization to the nucleus and the mitochondria,

Fig. 21 Reaction-based detection mechanism of probe **44** for GSH.
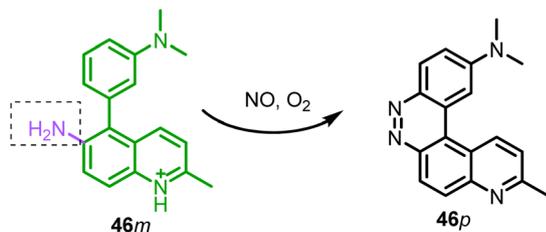
Fig. 22 Reaction-based sensing mechanism of probe **46** for NO detection.

respectively. In the presence of ctDNA, **46m** showed high sensitivity to NO (LOD = 2.8 nM). However, due to nucleus localization, **46p** could be an excellent green-fluorescent probe for the nucleus.

8.3 Nucleus DNA detection

The nucleus viscosity and G-quadruplex have several critical roles in biological processes, such as controlling gene expression, preventing tumorigenesis, *etc.* Thus, to better understand their molecular process and function, an efficient tool that can target the nucleus is in demand. Sun *et al.* developed D–π–A type probe **47** based on triphenylamine (donor) and *N*-methyl benzothiazole (acceptor and nucleus-targeting group) (Fig. 23, Table 1).[169] With a considerable ratiometric increase in fluorescence, probe **47** revealed strong selectivity to G-quadruplex DNA and viscosity inside the nucleus. However, the notable limitation of probe **47** is that it cannot distinguish between G-quadruplex DNA and viscosity change.

Ferroptosis controls cell death by accumulating lipid peroxide-associated reactive oxygen species, which is predicted to change the shape and polarity of lipid droplets (LDs). However, there needs to be concrete proof of this. Wang *et al.* reported dual-organelle targeting (LD and nucleus) fluorescent probe **48** for monitoring cellular microenvironment polarity change (Fig. 23, Table 1).[170] The fluorescence titration of probe **48** with ds26DNA revealed ~11-fold increase in emission intensity at 670 nm, while emission maxima at 470 nm remained constant. From molecular modeling calculations, the selectivity of probe **48** to DNA could be due to its binding to the
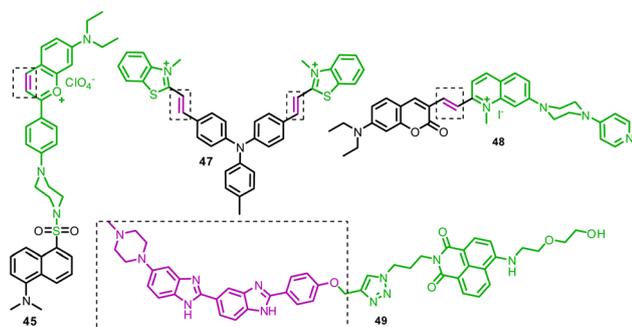
minor grooves of DNA through hydrogen bonding and electrostatic interactions.

Yang *et al.* developed a ratiometric fluorescent probe **49** based on a naphthalimide dye and a Hoechst (nucleus-targeting unit) (Fig. 23, Table 1).[171] Upon gradually increasing the concentration of ctDNA, the emission maxima of probe **49** at 450 nm and 505 nm increased significantly, ascribed to the FRET process from the Hoescht to the naphthalimide unit. Probe **49**'s remarkable benefit is its ability to provide precise and wash-free nuclear DNA staining in living cells, including normal cells COS-7 and L02, as well as cancer cells MCF-7, SMMC-7721, and HeLa. Furthermore, probe **49** found a potential application for monitoring nucleus DNA damage induced by the anticancer drug etoposide and hydroxyl radicals.

8.4 Challenges

For chemical biology purposes, nucleus-targeting systems have been thoroughly investigated. However, commercially available nucleus-targeting fluorescent probes are limited to staining DNAs.[172] Nowadays, newly developed nucleus-targeting probes are more specific to a particular analyte but are still rare. Furthermore, each developed method needs a clear explanation of organelle-specific/targeting mechanism, cellular toxicity, targeting ability in the altered environment, probe stability, response time, *etc.*

9 Membrane-targeting ratiometric fluorescent probes

Cytomembrane is an essential target for the study of dynamics and morphology due to the recent discovery of membrane microdomains (rafts) in cancer[173] and viral infection.[174,175] The cytomembrane also contributes to amyloid formation in neurodegenerative diseases.[176,177]

9.1 Reactive sulphur species (RSS) detection in the membrane

Zhang *et al.* developed probes **50** and **51** based on coumarin derivatives (Fig. 24, Table 1).[178] Notably, the fluorescence spectrum of probe **50** and **51** exhibited ratiometric response with SO$_2$ and visible color change of the solution from dark purple to colorless. The nucleophilic addition reaction was the sensing

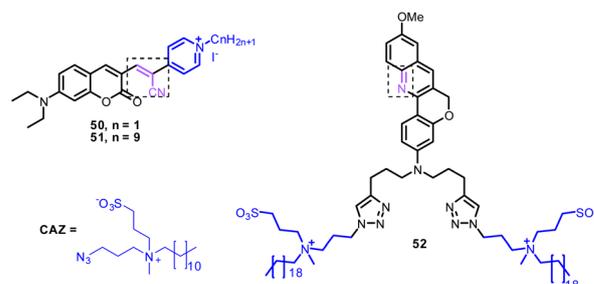Fig. 23 Chemical structure of nucleus-targeting ratiometric fluorescent probes **45–49**.

Fig. 24 Chemical structure of membrane-targeting ratiometric fluorescent probes **50–52**.

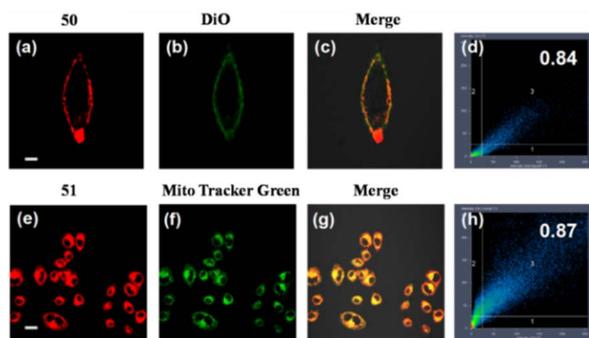© 2023 The Author(s). Published by the Royal Society of Chemistry

Fig. 25 Co-localization imaging of **50** and **51**. Fluorescence images of (a, e) **50** and **51** in the red channel; (b, f) MitoTracker Green in the green channel; (c, g) overlay image; (d, h) **50** and **51** intensity correlation plot. Reprinted from ref. 178, copyright 2021 Elsevier.

mechanism of probes **50** and **51** for SO$_2$. From cell imaging experiments, probes **50** and **51** exhibited good cytomembrane-targeting and mitochondrion-targeting ability and can detect SO$_2$ in mice. Due to the negatively charged cell inner membrane, the cationic property of probe **50** allowed it to target the cell membrane through electrostatic interactions. However, the probe **51** can selectively accumulate in mitochondria because of its positively charged nature, long alkyl chain, and appropriate hydrophobic characteristic (Fig. 25).

9.2 Monitoring pH changes in the membrane

The cell's various biomolecules, pathogens, and fluids are regulated by intracellular vesicles that the plasma membrane produces.[179] Intravesicular pH changes during trafficking depend on endosomal maturation and signaling.[180] The cell's various biomolecules, pathogens, and fluids are regulated by intracellular vesicles that the plasma membrane produces. Inspired by the work of Liu *et al.* on red-shifted chromenoqui-noline based probes,[181] Michelis *et al.* designed probe **52** based on chromenoquinoline for imaging the distribution and acidi-fication of intracellular vesicles and to measure the pH of individual vesicles (Fig. 24, Table 1).[182] From the fluorescence experiment, probe **52** underwent an increase in emission intensity upon binding with the plasma membrane (10-fold). Furthermore, probe **52** monitored the acidification of the vesi-cles throughout the endocytic pathway. The main limitation associated with probe **52** is that we cannot use it for long-term tracking due to the instability of the basic form.

9.3 Challenges

Despite several efforts in designing membrane-targeting ratio-metric fluorescent probes, literature reports are rare. To date, no commercially available membrane-targeting fluorescent probes are available. In the future, researchers must consider several parameters for designing efficient membrane-targeting fluorescent probes, such as probe stability, selectivity, sensi-tivity, response time, orientation/location in the membrane, and detailed mechanism of interaction with the membrane.

10 Multi organelle-targeting ratiometric fluorescent probes

Developing a powerful molecular tool that can target other organelles simultaneously is necessary to study the relationship between different organelles.

10.1 Reactive sulphur species (RSS) detection in lysosome and mitochondria

From a recent study, SO$_2$ is a critical gas messenger that plays a vital role in many cellular processes, including apoptosis in lysosomes and mitochondria. Therefore, to know the relation-ship between lysosome and mitochondria in regulating SO$_2$-related cellular activities, Kong *et al.* pioneered probe **53** (Fig. 26, Table 1).[183] Free probe **53** showed emission at 600 nm (red fluorescence) owing to the FRET process between the naphthalimide unit and the semi-cyanine unit. Upon the addition of SO$_2$, the emission intensity at 600 nm decreased. In comparison, a new emission maximum at 530 nm appeared and increased, assigned to Michael's addition reaction of SO$_2$ in the semi-cyanine unit and inhibition of the FRET process. In living cells, probe **53** found an application for simultaneously detecting endogenous SO$_2$ in lysosome and mitochondria by one and two-photon modes.

10.2 Monitoring pH fluctuation in mitochondria and lipid droplets (LDs)

Understanding the fundamental connection between fluctu-ating mitochondrial pH and lipid droplet (LD) generation is crucial for understanding cell physiology. Bai *et al.* developed probe **54** based on hemicyanine and rhodamine dyes for selectively monitoring mitochondria and lipid droplets under different pH values through a dual-emission channel (Fig. 27 and 28, Table 1).[19] The pH (from 2.52 to 10.50) sensing behavior of probe **54** revealed a notable decrease in the emission band at 580 nm, accompanied by the increase in a new emission peak at 450 nm, attributed to two different structural forms under acidic and basic medium. Under acidic conditions, the ring-open form of probe **54** targeted mitochondria and displayed solid red emission. In contrast, the ring-closed form of probe **54** targeted LDs and gave blue emission. Furthermore, applied probe **54** monitored the pH fluctuation in living cells in the presence of different exotic chemicals.

10.3 Challenges

Dual organelle-targeting probes hold great promise for eluci-dating the relationship between organelles and deepening our
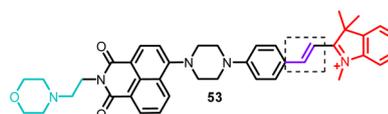

Fig. 26 Chemical structure of dual organelle-targeting ratiometric fluorescent probe **53**.
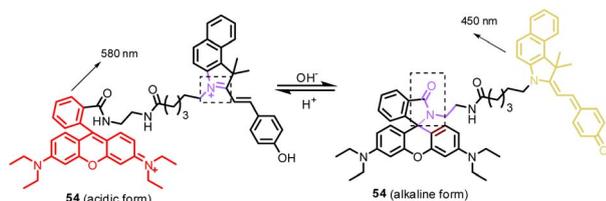
Fig. 27 Chemical structure of probe **54** and the proposed pH sensing mechanism.

Fig. 28 Organelle-targeting mechanism of probe **54**. Reprinted from ref. 19, copyright 2022 American Chemical Society.

understanding of the biological processes behind the biological species. However, building molecular probes with two or more sensitive moieties is challenging. Furthermore, dual organelle-targeting probes are rare in the literature.

11 Conclusion and future outlook

This review article highlighted recent advances in organelle-targeting ratiometric fluorescent probes reported since 2015. In particular, we discussed synthetic fluorescent probes with potential applications in biological systems such as biological species detection, fluorescence imaging, studying physiological and pathological processes, *etc.* Additionally, we highlighted the methods utilized to construct these probes and sensing mechanisms for their response to particular species.

Nowadays, significant research has been put into developing organelle-targeting fluorescent probes to create fluorescent tools with improved resolution and sensitivity and a better understanding of the molecular mechanisms behind various biological processes. In conclusion, high selectivity, high reactivity, fast response time, low detection limit, good solubility, and organelle-targeting ability are the multiple advantages of the fluorescent probe. Currently, ratiometric probes that meet all the above properties are rare in the literature.

Researchers will always be very interested in the advancement of ratiometric probes and their commercial applications. Despite the abundance of current outcomes, the following areas require additional work in the future. First, compared to traditional one-photon fluorescence probes, two-photon fluorescent probes provide several advantages, such as deep visualization, reduced photo-toxicity, minimal light scattering, and highly bright and contrast images.[184] Thus, the development of ratiometric probes with two-photon properties is greatly needed. Second, for *in vivo* application, near-infra-red (NIR) probes provide several

advantages, such as deep tissue penetration, reduced photon scattering, and reduced photodamage to the living organism.[185] Thus, ratiometric probes with emissions in the NIR region are in demand. Third, Reversible probes hold great promise for revealing the dynamic states of relevant analytes in various processes.[52] Thus, developing ratiometric probes for biological species detection based on reversible reactions is essential. Fourth, probes targeting organelles such as the nucleus, membrane, lipid droplet (LD), melanosome, and Golgi apparatus are rare in the literature (Table 1). Fifth, there are several species in biological systems. However, only a limited number of species, such as ROS, RNS, RSS, metal ions, and pH, have been the subject of interest (Table 1). Sixth, most of the discussed ratiometric probes have found applications for the bio-imaging of biological species in living cells and mice. To date, no commercially available ratiometric probes are available. By taking the factors mentioned above into account in the probe design, fluorescent probes can be utilized as significant materials in the coming days, and their commercial availability will be anticipated in the future.

Data availability

All the data were collected freely from websites such as **https://scholar.google.com/** and **https://www.sci-hub.se/**. Microsoft Office Word 2007 was used for writing the article, while Microsoft Office PowerPoint 2007 was used for graphical presentation. ChemBioDraw was used for chemical structure drawing.

Author contributions

Dr Manoj Kumar Goshisht and Dr Neetu Tripathi contributed equally to writing the original draft and to reviewing and editing the manuscript. Dr Goutam Kumar Patra and Dr Manohar Chaskar contributed to reviewing and editing the manuscript.

Conflicts of interest

The authors declare that they have no known competing financial interests or personal relationships that could have appeared to influence the work reported in this paper.

References

1 X. Chen, R. Kang, G. Kroeme and D. Tang, Organelle-specific regulation of ferroptosis, *Cell Death Differ.*, 2021, **28**, 2843–2856.

2 N. Trinh, K. A. Jolliffe and E. New, Dual-Functionalisation of Fluorophores for the Preparation of Targeted and Selective Probes, *Angew. Chem., Int. Ed.*, 2020, **59**, 20290–20301.

3 M. Schrader, M. Kamoshita and M. Islinger, Organelle interplay-peroxisome interactions in health and disease, *J. Inherited Metab. Dis.*, 2020, **43**, 71–89.

4 J. Lin, K. Yang and E. J. New, Strategies for organelle targeting of fluorescent probes, *Org. Biomol. Chem.*, 2021, **19**, 9339–9357.

5   Z. He, Y. Zhang, A. R. Khan, J. Ji, A. Yu and G. Zhai, A novel progress of drug delivery system for organelle targeting in tumour cells, *J. Drug Targeting*, 2020, **29**, 12–28.

6   Y. Chen, Y. Bai, Z. Han, W. He and Z. Guo, Photoluminescence imaging of Zn^{2+} in living systems, *Chem. Soc. Rev.*, 2015, **44**, 4517–4546.

7   N.-E. Choi, J.-Y. Lee, E.-C. Park, J.-H. Lee and J. Lee, Recent Advances in Organelle-Targeted Fluorescent Probes, *Molecules*, 2021, **26**, 217.

8   A. Bigdeli, F. Ghasemi, S. Abbasi-Moayed, M. Shahrajabian, N. Fahimi-Kashani, S. Jafarinejad, M. A. F. Nejad and M. R. Hormozi-Nezhad, Ratiometric fluorescent nanoprobes for visual detection: design principles and recent advances – a review, *Anal. Chim. Acta*, 2019, **1079**, 30–58.

9   S.-H. Park, N. Kwon, J.-H. Lee, J. Yoon and I. Shin, Synthetic ratiometric fluorescent probes for detection of ions, *Chem. Soc. Rev.*, 2020, **49**, 143–179.

10 X. Huang, J. Song, B. C. Yung, X. Huang, Y. Xiong and X. Chen, Ratiometric optical nanoprobes enable accurate molecular detection and imaging, *Chem. Soc. Rev.*, 2018, **47**, 2873–2920.

11 M. H. Lee, J. S. Kim and J. L. Sessler, Small molecule-based ratiometric fluorescence probes for cations, anions, and biomolecules, *Chem. Soc. Rev.*, 2015, **44**, 4185–4191.

12 P. Wu, X. Hou, J.-J. Xu and H.-Y. Chen, Ratiometric fluorescence, electrochemiluminescence, and photoelectrochemical chemo/biosensing based on semiconductor quantum dots, *Nanoscale*, 2016, **8**, 8427–8442.

13 S. Wu, H. Min, W. Shi and P. Cheng, Multicenter Metal–Organic Framework-Based Ratiometric Fluorescent Probes, *Adv. Mater.*, 2020, **32**, 1805871.

14 Q. Yuan, Z.-M. Zhao, Y.-R. Zhang, L. Su, J.-Y. Miao and B.-X. Zhao, A lysosome-targeted ratiometric fluorescent probe for detection of hypochlorous acid in living cells, *Sens. Actuators, B*, 2017, **247**, 736–741.

15 S.-L. Shen, X.-Q. Huang, X.-H. Lin and X.-Q. Cao, A ratiometric fluorescent probe for lysosomal hypochlorous acid based on through-bond energy transfer strategy, *Anal. Chim. Acta*, 2019, **1052**, 124–130.

16 F. Ghasemi, M. R. Hormozi-Nezhad and M. Mahmoudi, A new strategy to design colorful ratiometric probes and its application to fluorescent detection of Hg(II), *Sens. Actuators, B*, 2018, **259**, 894–899.

17 B. Liu, F. Zeng, G. Wu and S. Wu, Nanoparticles as scaffolds for FRET-based ratiometric detection of mercury ions in water with QDs as donors, *Analyst*, 2012, **137**, 3717–3724.

18 Y. L. Pak, S. J. Park, G. Song, Y. Yim, H. Kang, H. M. Kim, J. Bouffard and J. Yoon, Endoplasmic Reticulum-Targeted Ratiometric N-Heterocyclic Carbene Borane Probe for Two-Photon Microscopic Imaging of Hypochlorous Acid, *Anal. Chem.*, 2018, **90**, 12937–12943.

19 Q. Bai, C. Yang, M. Yang, Z. Pei, X. Zhou, J. Liu, H. Ji, G. Li, M. Wu, Y. Qin, Q. Wang and L. Wu, pH-Dominated Selective Imaging of Lipid Droplets and Mitochondria via a Polarity-Reversible Ratiometric Fluorescent Probe, *Anal. Chem.*, 2022, **94**, 2901–2911.

20 M. Ren, K. Zhou, L. He and W. Lin, Mitochondria and lysosome-targetable fluorescent probes for HOCl: recent advances and perspectives, *J. Mater. Chem. B*, 2018, **6**, 1716–1733.

21 X.-Z. Yang, X.-R. Wei, R. Sun, Y.-J. Xu and J.-F. Ge, A novel xanthylene-based effective mitochondria-targeting ratiometric cysteine probe and its bioimaging in living cells, *Talanta*, 2020, **209**, 120580.

22 G. Cheng, J. Fan, W. Sun, K. Sui, X. Jin, J. Wang and X. Peng, A highly specific BODIPY-based probe localized in mitochondria for HClO imaging, *Analyst*, 2013, **138**, 6091–6096.

23 Q. Huang, Y. Zhou, Q. Zhang, E. Wang, Y. Min, H. Qiao, J. Zhang and T. Ma, A new "off–on" fluorescent probe for Pd^{2+} in aqueous solution and live-cell based on spirolactam ring-opening reaction, *Sens. Actuators, B*, 2015, **208**, 22–29.

24 J. Liu, X. Liu, S. Lu, L. Zhang, L. Feng, S. Zhong, N. Zhang, T. Bing and D. Shangguan, Ratiometric detection and imaging of hydrogen sulfide in mitochondria based on a cyanine/naphthalimide hybrid fluorescent probe, *Analyst*, 2020, **145**, 6549–6555.

25 X. Zhang, G. J. Song, X. J. Cao, J. T. Liu, M. Y. Chen, X. Q. Cao and B.-X. Zhao, A new fluorescent pH probe for acidic conditions, *RSC Adv.*, 2015, **5**, 89827–89832.

26 J. Yang, K. Li, J.-T. Hou, L.-L. Li, C.-Y. Lu, Y.-M. Xie, X. Wang and X.-Q. Yu, Novel Tumor-Specific and Mitochondria-Targeted near-Infrared-Emission Fluorescent Probe for SO_2 Derivatives in Living Cells, *ACS Sens*, 2016, **2**, 166–172.

27 J.-T. Hou, M.-Y. Wu, K. Li, J. Yang, K.-K. Yu, Y.-M. Xie and X.-Q. Yu, Mitochondria-targeted colorimetric and fluorescent probes for hypochlorite and their applications for *in vivo* imaging, *Chem. Commun.*, 2014, **50**, 8640–8643.

28 L. Zang, C. Liang, Y. Wang, W. Bu, H. Sun and S. Jiang, A highly specific pyrene-based fluorescent probe for hypochlorite and its application in cell imaging, *Sens. Actuators, B*, 2015, **211**, 164–169.

29 L. Wang, M. Ren, Z. Li, L. Dai and W. Lin, Development of a FRET-based ratiometric fluorescent probe to monitor the changes in palladium(II) in aqueous solution and living cells, *New J. Chem.*, 2019, **43**, 552.

30 P. Gao, W. Pan, N. Li and B. Tang, Fluorescent probes for organelle-targeted biological species imaging, *Chem. Sci.*, 2019, **10**, 6035–6071.

31 Z. Xue, R. Zhu, S. Wang, J. Li, J. Han, J. Liu and S. Han, Organelle-Directed Staudinger Reaction Enabling Fluorescence-on Resolution of Mitochondrial Electropotentials via a Self-Immolative Charge Reversal Probe, *Anal. Chem.*, 2018, **90**, 2954–2962.

32 T. B. Ren, Q. L. Zhang, D. Su, X. X. Zhang, L. Yuan and X. B. Zhang, Detection of analytes in mitochondria without interference from other sites based on an innovative ratiometric fluorophore, *Chem. Sci.*, 2018, **9**, 5461–5466.

33 Y. Chen, C. Zhu, J. Cen, Y. Bai, W. He and Z. Guo, Ratiometric detection of pH fluctuation in mitochondria with a new fluorescein/cyanine hybrid probe, *Chem. Sci.*, 2015, **6**, 3187–3194.

34 X. Zhang, B. Wang, C. Wang, L. Chen and Y. Xiao, Monitoring Lipid Peroxidation within Foam Cells by Lysosome-Targetable and Ratiometric Probe, *Anal. Chem.*, 2015, **87**, 8292–8300.

35 Z. Wu, D. Liang and X. Tang, Visualizing Hydrogen Sulfide in Mitochondria and Lysosome of Living Cells and in Tumors of Living Mice with Positively Charged Fluorescent Chemoprobes, *Anal. Chem.*, 2016, **88**, 9213–9218.

36 Y. Cai, C. Gui, K. Samedov, H. Su, X. Gu, S. Li, W. Luo, H. H. Y. Sung, J. W. Y. Lam, R. T. K. Kwok, I. D. Williams, A. Qin and B. Z. Tang, An acidic pH independent piperazine-TPE AIEgen as a unique bioprobe for lysosome tracing, *Chem. Sci.*, 2017, **8**, 7593.

37 R. Zhou, Q. Peng, D. Wan, C. Yu, Y. Zhang, Y. Hou, Q. Luo, X. Li, S. Zhang, L. Xie, P. Ou and Y. Peng, Construction of a lysosome-targetable ratiometric fluorescent probe for H_2O_2 tracing and imaging in living cells and an inflamed model, *RSC Adv.*, 2021, **11**, 24032.

38 L. Fang, G. Trigiante, R. Crespo-Otero, C. S. Hawes, M. P. Philpott, C. R. Jones and M. Watkinson, Endoplasmic reticulum targeting fluorescent probes to image mobile Zn^{2+}, *Chem. Sci.*, 2019, **10**, 10881–10887.

39 J.-T. Hou, H. S. Kim, C. Duan, M. S. Ji, S. Wang, L. Zeng, W. X. Ren and J. S. Kim, A ratiometric fluorescent probe for detecting hypochlorite in the endoplasmic reticulum, *Chem. Commun.*, 2019, **55**, 2533–2536.

40 B. Dong, W. Song, Y. Lu, X. Kong, A. H. Mehmood and W. Lin, An ultrasensitive ratiometric fluorescent probe based on the ICT-PET-FRET mechanism for the quantitative measurement of pH values in the endoplasmic reticulum (ER), *Chem. Commun.*, 2019, **55**, 10776–10779.

41 Q. Ma, C. Wang, G. Mao, M. Tian, J. Suna and S. Feng, An endoplasmic reticulum-targeting and ratiometric fluorescent probe for hypochlorous acid in living cells based on a 1,8-naphthalimide derivative, *New J. Chem.*, 2020, **44**, 18389–18398.

42 J. Colston, R. Horobin, F. Rashid-Doubell, J. Pediani and K. K. Johal, Why fluorescent probes for endoplasmic reticulum are selective: an experimental and QSAR-modelling study, *Biotech. Histochem.*, 2003, **78**, 323–332.

43 L. Zhou, Z.-Q. Cheng, N. Li, Y.-X. Gea, H.-X. Xie, K. Zhu, A. Zhou, J. Zhang, K.-M. Wang and C.-S. Jiang, A highly sensitive endoplasmic reticulum-targeting fluorescent probe for the imaging of endogenous H_2S in live cells, *Spectrochim. Acta, Part A*, 2020, **240**, 118578.

44 T. Yang, J. Sun, W. Yao and F. Gao, A two-photon fluorescent probe for turn-on monitoring HOCl level in endoplasmic reticulum, *Dyes Pigm.*, 2020, **180**, 108435.

45 W. Zhang, J. Zhang, P. Li, J. Liu, D. Su and B. Tang, Two-photon fluorescence imaging reveals a Golgi apparatus superoxide anion-mediated hepatic ischaemia-reperfusion signalling pathway, *Chem. Sci.*, 2018, **10**, 879–883.

46 R. S. Li, P. F. Gao, H. Z. Zhang, L. L. Zheng, C. M. Li, J. Wang, Y. F. Li, F. Liu, N. Li and C. Z. Huang, Chiral nanoprobes for targeting and long-term imaging of the Golgi apparatus, *Chem. Sci.*, 2017, **8**, 6829–6835.

47 P. Li, X. Guo, X. Bai, X. Wang, Q. Ding, W. Zhang, W. Zhang and B. Tang, Golgi Apparatus Polarity Indicates Depression-Like Behaviors of Mice Using in Vivo Fluorescence Imaging, *Anal. Chem.*, 2019, **91**, 3382–3388.

48 T. Hirayama, M. Inden, H. Tsuboi, M. Niwa, Y. Uchida, Y. Naka, I. Hozumi and H. Nagasawa, A Golgi-targeting fluorescent probe for labile Fe(II) to reveal an abnormal cellular iron distribution induced by dysfunction of VPS35, *Chem. Sci.*, 2019, **10**, 1514–1521.

49 M. W. Hetzer, The Nuclear Envelope, *Perspect. Biol.*, 2010, **2**, a000539.

50 A. Nakamura, K. Takigawa, Y. Kurishita, K. Kuwata, M. Ishida, Y. Shimoda, I. Hamachi and S. Tsukiji, Hoechst tagging: a modular strategy to design synthetic fluorescent probes for live-cell nucleus imaging, *Chem. Commun.*, 2014, **50**, 6149–6152.

51 G. Lukinavicius, C. Blaukopf, E. Pershagen, A. Schena, L. Reymond, E. Derivery, M. Gonzalez-Gaitan, E. D'Este, S. W. Hell, D. W. Gerlich and K. Johnsson, SiR–Hoechst is a far-red DNA stain for live-cell nanoscopy, *Nat. Commun.*, 2015, **6**, 8497.

52 Y. Ma, W. Gao, L. Zhu, Y. Zhao and W. Lin, A ratiometric fluorescent probe for reversible monitoring of endogenous SO_2/formaldehyde in cytoplasm and nucleoli regions and its applications in living mice, *Analyst*, 2020, **145**, 1865–1870.

53 S. Zhang, H. Sun, H. Chen, Q. Li, A. Guan, L. Wang, Y. Shi, S. Xu, M. Liu and Y. Tang, Direct visualization of nucleolar G-quadruplexes in live cells by using a fluorescent light-up probe, *Biochim. Biophys. Acta, Gen. Subj.*, 2018, **1862**, 1101–1106.

54 N. Sato, G. Tsuji, Y. Sasaki, A. Usami, T. Moki, K. Onizuka, K. Yamada and F. Nagatsugi, A new strategy for site-specific alkylation of DNA using oligonucleotides containing an abasic site and alkylating probes, *Chem. Commun.*, 2015, **51**, 14885–14888.

55 M. K. Goshisht and N. Tripathi, Fluorescence-based probes as an emerging tool for anion detection: mechanism, probey materials and applications, *J. Mater. Chem. C*, 2021, **9**, 9820–9850.

56 M. K. Goshisht, G. K. Patra and N. Tripathi, Fluorescent Schiff base probes as a versatile tool for metal ion detection: strategies, mechanistic insights, and applications, *Mater. Adv.*, 2022, **3**, 2612–2669.

57 N. Tripathi and M. K. Goshisht, *Aggregation of Luminophores in Supramolecular Systems: From Mechanisms to Applications*, CRC Press, Taylor Fr., 2020, pp. 1–220.

58 Z. Liu, W. He and Z. Guo, Metal coordination in photoluminescent sensing, *Chem. Soc. Rev.*, 2013, **42**, 1568–1600.

59 J. Gong, C. Liu, X. Jiao, S. He, L. Zhao and X. Zeng, Novel mitochondria-targeted viscosity probe based on a fluorescent rotatable xanthene-hemicyanine dyad, *Microchem. J.*, 2020, **158**, 105191.

60 W. Sun, Y.-D. Shi, A.-X. Ding, Z.-L. Tan, H. Chen, R. Liu, R. Wang and Z.-L. Lu, Imaging viscosity and peroxynitrite by a mitochondria-targeting two-photon ratiometric fluorescent probe, *Sens. Actuators, B*, 2018, **276**, 238–246.

61 K. Yang, J. L. Kolanowski and E. J. New, Mitochondrially targeted fluorescent redox probes, *Interface Focus*, 2017, **7**, 20160105.

62 G. Zhang, J. J. Gruskos, M. S. Afzal and D. Buccella, Visualizing changes in mitochondrial Mg^{2+} during apoptosis with organelle-targeted triazole-based ratiometric fluorescent probes, *Chem. Sci.*, 2015, **6**, 6841.

63 Z. M. Prokopowicz, F. Arce, R. Biedron, C. L. Chiang, M. Ciszek, D. R. Katz, M. Nowakowska, S. Zapotoczny, J. Marcinkiewic and B. M. Chain, Hypochlorous Acid: A Natural Adjuvant That Facilitates Antigen Processing, Cross-Priming, and the Induction of Adaptive Immunity, *J. Immunol.*, 2010, **184**, 824–835.

64 N. Tripathi and M. K. Goshisht, Recent Advances and Mechanistic Insights into Antibacterial Activity, Antibiofilm Activity, and Cytotoxicity of Silver Nanoparticles, *ACS Appl. Bio Mater.*, 2022, **5**, 1391–1463.

65 Q. Hu, C. Qin, L. Huang, H. Wang, Q. Liu and L. Zeng, Selective visualization of hypochlorite and its fluctuation in cancer cells by a mitochondria-targeting ratiometric fluorescent probe, *Dyes Pigm.*, 2018, **149**, 253–260.

66 M. Valko, D. Leibfritz, J. Moncol, M. T. Cronin, M. Mazur and J. Telser, Free radicals and antioxidants in normal physiological functions and human disease, *Int. J. Biochem. Cell Biol.*, 2007, **39**, 44.

67 B. D'Autréaux and M. B. Toledano, ROS as signalling molecules: mechanisms that generate specificity in ROS homeostasis, *Nat. Rev. Mol. Cell Biol.*, 2007, **8**, 813–824.

68 N. Li, J. Huang, Q. Wang, Y. Gu and P. Wang, A reaction based one- and two-photon fluorescent probe for selective imaging H_2O_2 in living cells and tissues, *Sens. Actuators, B*, 2018, **254**, 411–416.

69 A. M. Shah and K. M. Channon, Free radicals and redox signalling in cardiovascular disease, *Heart*, 2004, **90**, 486–487.

70 L. He, X. Liu, Y. Zhang, L. Yang, Q. Fang, Y. Geng, W. Chen and X. Song, A mitochondria-targeting ratiometric fluorescent probe for imaging hydrogen peroxide with long-wavelength emission and large Stokes shift, *Sens. Actuators, B*, 2018, **276**, 247–253.

71 S.-L. Shen, X.-F. Zhang, Y.-Q. Ge, Y. Zhua and X.-Q. Cao, A mitochondria-targeting ratiometric fluorescent probe for the detection of hypochlorite based on the FRET strategy, *RSC Adv.*, 2017, **7**, 55296.

72 C. Han, H. Yang, M. Chen, Q. Su, W. Feng and F. Li, Mitochondria-Targeted Near-Infrared Fluorescent Off–On Probe for Selective Detection of Cysteine in Living Cells and *in vivo*, *ACS Appl. Mater. Interfaces*, 2015, **7**, 27968–27975.

73 Y. Zhou and J. Yoon, Recent progress in fluorescent and colorimetric chemoprobes for detection of amino acids, *Chem. Soc. Rev.*, 2012, **41**, 52–67.

74 D. W. Bak and E. Weerapana, Cysteine-mediated redox signalling in the mitochondria, *Mol. BioSyst.*, 2015, **11**, 678–697.

75 S. Y. Lim, K. H. Hong, D. I. Kim, H. Kwon and H. J. Kim, Tunable heptamethine-azo dye conjugate as an NIR fluorescent probe for the selective detection of mitochondrial glutathione over cysteine and homocysteine, *J. Am. Chem. Soc.*, 2014, **136**, 7018–7025.

76 W. Niu, L. Guo, Y. Li, S. Shuang, C. Dong and M. S. Wong, Highly Selective Two-Photon Fluorescent Probe for Ratiometric Sensing and Imaging Cysteine in Mitochondria, *Anal. Chem.*, 2016, **88**, 1908–1914.

77 K. R. Olson, Hydrogen sulfide, reactive sulfur species and coping with reactive oxygen species, *Free Radical Biol. Med.*, 2019, **140**, 74–83.

78 J. Beltowski, G. Wojcicka and A. Jamroz-Wisniewska, Hydrogen sulfide in the regulation of insulin secretion and insulin sensitivity: implications for the pathogenesis and treatment of diabetes mellitus, *Biochem. Pharmacol.*, 2018, **149**, 60–76.

79 C. Szabo, C. Coletta, C. Chao, K. Modis, B. Szczesny, A. Papapetropoulos and M. R. Hellmich, Tumor-derived hydrogen sulfide, produced by cystathionine-β-synthase, stimulates bioenergetics, cell proliferation, and angiogenesis in colon cancer, *Proc. Natl. Acad. Sci. U. S. A.*, 2013, **110**, 12474–12479.

80 L. Zhou, L. Xie, C. Liu and Y. Xiao, New trends of molecular probes based on the fluorophore 4-amino-1,8-naphthalimide, *Chin. Chem. Lett.*, 2019, **30**, 1799–1808.

81 Q. Han, L. Yang, Y. Song, J. Ru, H. Zhang, H. Jiang and X. Wang, A ratiometric fluorescent probe for monitoring the changes in the level of hydrogen polysulfides in mitochondria during stimulus-induced redox imbalance, *Dyes Pigm.*, 2021, **188**, 109190.

82 F. Pannullo, D. Lee, L. Neal, M. Dalvi, P. Agnew, F. M. Connor and C. Sarran, Scoping the proximal and distal dimensions of climate change on health and wellbeing, *Environ. Health*, 2017, **16**, 29.

83 A. Salurcan, M. Turkyilmaz and M. Ozkan, Effects of sulfur dioxide concentration on organic acids and β-carotene in dried apricots during storage, *Food Chem.*, 2017, **221**, 412–421.

84 S. C. Morgan, C. M. Scholl, N. L. Benson, M. L. Stone and D. M. Durall, Sulfur dioxide addition at crush alters *Saccharomyces cerevisiae* strain composition in spontaneous fermentations at two Canadian wineries, *Int. J. Food Microbiol.*, 2017, **244**, 96–102.

85 R. Nassar, A. Trivella, S. Mokh, M. Al-Iskandarani, H. Budzinski and P. Mazellier, Photodegradation of sulfamethazine, sulfamethoxypiridazine, amitriptyline, and clomipramine drugs in aqueous media, *J. Photochem. Photobiol., A*, 2017, **336**, 176–182.

86 Y. Zhang, L. Guan, H. Yu, Y. Yan, L. Du, Y. Liu, M. Sun, D. Huang and S. Wang, Reversible Fluorescent Probe for

Selective Detection and Cell Imaging of Oxidative Stress Indicator Bisulfite, *Anal. Chem.*, 2016, **88**, 4426–4431.

87 Y. Sun, S. Fan, S. Zhang, D. Zhao, L. Duan and R. Li, A fluorescent turn-on probe based on benzo[*e*]indolium for bisulfite through 1,4-addition reaction, *Sens. Actuators, B*, 2014, **193**, 173–177.

88 Y. Huang, Y. Zhang, F. Huo and C. Yin, FRET-dependent single/two-channel switch endowing a dual detection for sulfite and its organelle targeting applications, *Dyes Pigm.*, 2021, **184**, 108869.

89 Y. Liu, K. Li, M. -Y. Wu, Y. -H. Liu, Y. -M. Xie and X. -Q. Yu, A mitochondria-targeted colorimetric and ratiometric fluorescent probe for biological SO_2 derivatives in living cells, *Chem. Commun.*, 2015, **51**, 10236–10239.

90 Y. Liu, K. Li, K.-X. Xie, L.-L. Li, K.-K. Yu, X. Wang and X.-Q. Yu, A water-soluble and fast-response mitochondria-targeted fluorescent probe for colorimetric and ratiometric sensing of endogenously generated SO_2 derivatives in living cells, *Chem. Commun.*, 2016, **52**, 3430–3433.

91 Y. Wang, Q. Meng, R. Zhang, H. Jia, X. Zhang and Z. Zhang, A ratiometric fluorescence probe for imaging sulfur dioxide derivatives in the mitochondria of living cells, *Org. Biomol. Chem.*, 2017, **15**, 2734–2739.

92 X.-B. Wang, H.-J. Li, Z. Chi, X. Zhao and Y.-C. Wu, A novel mitochondrial-targeted two-photon fluorescent probe for ultrafast monitoring of SO_2 derivatives and its applications, *Talanta*, 2020, **217**, 121086.

93 X.-B. Wang, H.-J. Li, Z. Chi, X. Zeng, L.-J. Wang, Y.-F. Cheng and Y.-C. Wu, A novel mitochondrial targeting fluorescent probe for ratiometric imaging SO_2 derivatives in living cells, *J. Photochem. Photobiol., A*, 2020, **390**, 112339.

94 W.-L. Wu, H.-L. Ma, M.-F. Huang, J.-Y. Miao and B.-X. Zhao, Mitochondria-targeted ratiometric fluorescent probe based on FRET for bisulfite, *Sens. Actuators, B*, 2017, **241**, 239–244.

95 J. Xu, J. Pan, X. Jiang, C. Qin, L. Zeng, H. Zhang and J. F. Zhang, A mitochondria-targeted ratiometric fluorescent probe for rapid, sensitive and specific detection of biological SO_2 derivatives in living cells, *Biosens. Bioelectron.*, 2016, **77**, 725–732.

96 L.-J. Zhang, Z.-Y. Wang, J.-T. Liu, J.-Y. Miao and B.-X. Zhao, A rational design of ratiometric fluorescent probes based on new ICT/FRET platform and imaging of endogenous sulfite in living cell, *Sens. Actuators, B*, 2017, **253**, 19–26.

97 M. Zhao, D. Liu, L. Zhou, B. Wu, X. Tian, Q. Zhang, H. Zhou, J. Yang, J. Wu and Y. Tian, Two water-soluble two-photon fluorescence probes for ratiometric imaging endogenous SO_2 derivatives in mitochondria, *Sens. Actuators, B*, 2018, **255**, 1228–1237.

98 X.-L. Zheng, H. Li, W. Feng, H.-C. Xia and Q.-H. Song, Two-Step Sensing, Colorimetric and Ratiometric Fluorescent Probe for Rapid Detection of Bisulfite in Aqueous Solutions and in Living Cells, *ACS Omega*, 2018, **3**, 11831–11837.

99 P. B. Mahaboob and S. M. Saumya, Suppression of mitochondrial oxidative phosphorylation and TCA enzymes in discrete brain regions of mice exposed to high

fluoride: Amelioration by Panax ginseng (Ginseng) and Lagerstroemia speciosa (Banaba) extracts, *Cell. Mol. Neurobiol.*, 2013, **33**, 453–464.

100 Y. Shen, X. Zhang, Y. Zhang, H. Li and Y. Chen, An ICT-Modulated strategy to construct colorimetric and ratiometric fluorescent probe for mitochondria-targeted fluoride ion in cell living, *Sens. Actuators, B*, 2018, **258**, 544–549.

101 R. Balamurugan, J.-H. Liu and B.-T. Liu, A review of recent developments in fluorescent probes for the selective detection of palladium ions, *Coord. Chem. Rev.*, 2018, **376**, 196–224.

102 L. Zhang, Y. Wang, J. Yu, G. Zhang, X. Cai, Y. Wu and L. Wang, A colorimetric and fluorescent probe based on PBIs for palladium detection, *Tetrahedron Lett.*, 2013, **54**, 4019–4022.

103 R. M. Perera and R. Zoncu, The Lysosome as a Regulatory Hub, *Annu. Rev. Cell Dev. Biol.*, 2016, **32**, 223–253.

104 M. Ren, B. Deng, K. Zhou, X. Kong, J. Y. Wang and W. Lin, Single Fluorescent Probe for Dual-Imaging Viscosity and H_2O_2 in Mitochondria with Different Fluorescence Signals in Living Cells, *Anal. Chem.*, 2017, **89**, 552.

105 J. Liu, S. Zhou, J. Ren, C. Wu and Y. Zhao, A lysosome-locating and acidic pH-activatable fluorescent probe for visualizing endogenous H_2O_2 in lysosomes, *Analyst*, 2017, **142**, 4522.

106 Z. Wu, M. Liu, Z. Liu and Y. Tian, Real-Time Imaging and Simultaneous Quantification of Mitochondrial H_2O_2 and ATP in Neurons with a Single Two-Photon Fluorescence-Lifetime-Based Probe, *J. Am. Chem. Soc.*, 2020, **142**, 7532.

107 Y. R. Zhang, N. Meng, J. Y. Miao and B. X. Zhao, A Ratiometric Fluorescent Probe Based on a Through-Bond Energy Transfer (TBET) System for Imaging HOCl in Living Cells, *Chem.–Eur. J.*, 2015, **21**, 19058–19063.

108 S. L. Shen, J. Y. Ning, X. F. Zhang, J. Y. Miao and B. X. Zhao, Through-bond energy transfer-based ratiometric fluorescent probe for the imaging of HOCl in living cells, *Sens. Actuators, B*, 2017, **244**, 907–913.

109 J. Liu, P. Niu, Y. Rong, W. Chen, X. Liu, L. Wei and X. Song, A phenothiazine coumarin based ratiometric fluorescent probe for real-time detection of lysosomal hypochlorite in living cell and zebra fish, *Spectrochim. Acta, Part A*, 2021, **261**, 120024.

110 D. Q. Rich, J. Schwartz, M. A. Mittleman, M. Link, H. Luttmann-Gibson, P. J. Catalano, F. E. Speizer and D. W. Dockery, Association of short-term ambient air pollution concentrations and ventricular arrhythmias, *Am. J. Epidemiol.*, 2005, **161**, 1123.

111 T.-M. Chen, W. G. Kuschner, J. Gokhale and S. Shofer, Outdoor air pollution: nitrogen dioxide, sulfur dioxide, and carbon monoxide health effects, *Am. J. Med. Sci.*, 2007, **333**, 249.

112 J. Chao, Y. Zhang, H. Wang, Y. Zhang, F. Huo, C. Yin, L. Qin and Y. Wang, Fluorescent Red GK as a fluorescent probe for selective detection of bisulfite anions, *Sens. Actuators, B*, 2013, **188**, 200–206.

113 Y.-Q. Sun, J. Liu, J. Zhang, T. Yang and W. Guo, Fluorescent probe for biological gas SO_2 derivatives bisulfite and sulfite, *Chem. Commun.*, 2013, **49**, 2637.

114 U. Tamima, M. Santra, C. W. Song, Y. J. Reo and K. H. Ahn, A Benzopyronin-Based Two-Photon Fluorescent Probe for Ratiometric Imaging of Lysosomal Bisulfite with Complete Spectral Separation, *Anal. Chem.*, 2019, **91**, 10779–10785.

115 V. S. Lin, W. Chen, M. Xian and C. J. Chang, Chemical probes for molecular imaging and detection of hydrogen sulfide and reactive sulfur species in biological systems, *Chem. Soc. Rev.*, 2015, **44**, 4596–4618.

116 B. Arunachalam, U. T. Phan, H. J. Geuze and P. Cresswell, Enzymatic reduction of disulfide bonds in lysosomes: Characterization of a Gamma-interferon-inducible lysosomal thiol reductase (GILT), *Proc. Natl. Acad. Sci. U. S. A.*, 2000, **97**, 745–750.

117 U. Tamima, C. W. Song, M. Santra, Y. J. Reo, H. Bannac, M. R. Islamd and K. H. Ahna, A benzo[*b*]xanthene-derived fluorescent probe capable of two-photon ratiometric imaging of lysosomal cysteine with high specificity, *Sens. Actuators, B*, 2020, **322**, 128588.

118 J. Zhang, R. Wang, Z. Zhu, L. Yi and Z. Xi, A FRET-based ratiometric fluorescent probe for visualizing H_2S in lysosomes, *Tetrahedron*, 2015, **71**, 8572–8576.

119 P. Verwilst, K. Sunwoo and J. S. Kim, The role of copper ions in pathophysiology and fluorescent probes for the detection thereof, *Chem. Commun.*, 2015, **51**, 5556.

120 S. G. Kaler, ATP7A-related copper transport diseases-emerging concepts and future trends, *Nat. Rev. Neurol.*, 2011, **7**, 15.

121 S. Lutsenko, A. Gupta, J. L. Burkhead and V. Zuzel, Cellular multitasking: the dual role of human Cu-ATPases in cofactor delivery and intracellular copper balance, *Arch. Biochem. Biophys.*, 2008, **476**, 22.

122 D. G. Barceloux, Copper, *Clin. Toxicol.*, 1999, **37**, 217.

123 C. Liu, X. Jiao, S. He, L. Zhao and X. Zeng, A highly selective and sensitive fluorescent probe for Cu^{2+} based on a novel naphthalimide–rhodamine platform and its application in live cell imaging, *Org. Biomol. Chem.*, 2017, **15**, 3947.

124 V. Dujols, F. Ford and A. W. Czarnik, A Long-Wavelength Fluorescent Chemodosimeter Selective for Cu(II) Ion in Water, *J. Am. Chem. Soc.*, 1997, **119**, 7386–7387.

125 W.-N. Wu, H. Wu, R.-B. Zhong, Y. Wang, Z.-H. Xu, X.-L. Zhao, Z.-Q. Xu and Y.-C. Fan, Ratiometric fluorescent probe based on pyrrole-modified rhodamine 6G hydrazone for the imaging of Cu^{2+} in lysosomes, *Spectrochim. Acta, Part A*, 2019, **212**, 121–127.

126 Y. Wang, L. Zhang, X. Han, L. Zhang, X. Wang and L. Chen, Fluorescent probe for mercury ion imaging analysis: strategies and applications, *Chem. Eng. J.*, 2021, **406**, 127166.

127 Y. Zhang, H. Chen, D. Chen, D. Wu, Z. Chen, J. Zhang, X. Chen, S. H. Liu and J. Yin, A colorimetric and ratiometric fluorescent probe for mercury (II) in lysosome, *Sens. Actuators, B*, 2016, **224**, 907–914.

128 Q. Xia, X. Wang, Y. Liu, Z. Shen, Z. Ge, H. Huang, X. Li and Y. Wang, An endoplasmic reticulum-targeted two-photon fluorescent probe for bioimaging of HClO generated during sleep deprivation, *Spectrochim. Acta, Part A*, 2020, **229**, 117992.

129 M. Yan, H. Fang, X. Wang, J. Xu, C. Zhang, L. Xu and L. Li, A two-photon fluorescent probe for visualizing endoplasmic reticulum peroxynitrite in Parkinson's disease models, *Sens. Actuators, B*, 2021, **328**, 129003.

130 H. Xiao, P. Li, X. Hu, X. Shi, W. Zhang and B. Tang, Simultaneous fluorescence imaging of hydrogen peroxide in mitochondria and endoplasmic reticulum during apoptosis, *Chem. Sci.*, 2016, **7**, 6153–6159.

131 C. Gao, Y. Tian, R. Zhang, J. Jing and X. Zhang, Endoplasmic Reticulum-Directed Ratiometric Fluorescent Probe for quantitative Detection of Basal H_2O_2, *Anal. Chem.*, 2017, **89**, 12945–12950.

132 L. Yuan, W. Lin, J. Song and Y. Yang, Development of an ICT-based ratiometric fluorescent hypochlorite probe suitable for living cell imaging, *Chem. Commun.*, 2011, **47**, 12691–12693.

133 G. Li, Q. Lin, L. Sun, C. Feng, P. Zhang, B. Yu, Y. Chen, Y. Wen, H. Wang, L. Ji and H. Chao, A mitochondrial targeted two-photon iridium(III) phosphorescent probe for selective detection of hypochlorite in live cells and *in vivo*, *Biomaterials*, 2015, **53**, 285–295.

134 H. Feng, Z. Zhang, Q. Meng, H. Jia, Y. Wang and R. Zhang, Rapid Response Fluorescence Probe Enabled In Vivo Diagnosis and Assessing Treatment Response of Hypochlorous Acid-Mediated Rheumatoid Arthritis, *Adv. Sci.*, 2018, **5**, 1800397.

135 S. Xu, H.-W. Liu, X.-X. Hu, S.-Y. Huan, J. Zhang, Y.-C. Liu, L. Yuan, F.-L. Qu, X.-B. Zhang and W. Tan, Visualization of Endoplasmic Reticulum Aminopeptidase 1 under Different Redox Conditions with a Two-Photon Fluorescent Probe, *Anal. Chem.*, 2017, **89**, 7641–7648.

136 Q. Ma, C. Wang, Y. Bai, J. Xu, J. Zhang, Z. Li and X. Guo, A lysosome-targetable and ratiometric fluorescent probe for hypochlorous acid in living cells based on a 1,8-naphthalimide derivative, *Spectrochim. Acta, Part A*, 2019, **223**, 117334.

137 Z. Guo, I. Shin and J. Yoon, Recognition and sensing of various species using boronic acid derivatives, *Chem. Commun.*, 2012, **48**, 5956–5967.

138 X. Sun, Q. Xu, G. Kim, S. E. Flower, J. P. Lowe, J. Yoon, J. S. Fossey, X. Qian, S. D. Bull and T. D. James, A water-soluble boronate-based fluorescent probe for the selective detection of peroxynitrite and imaging in living cells, *Chem. Sci.*, 2014, **5**, 3368–3373.

139 Q. Xu, K.-A. Lee, S. Lee, K. M. Lee, W.-J. Lee and J. Yoon, A Highly Specific Fluorescent Probe for Hypochlorous Acid and Its Application in Imaging Microbe-Induced HOCl Production, *J. Am. Chem. Soc.*, 2013, **135**, 9944–9949.

140 H. Li, Q. Yao, J. Fan, J. Du, J. Wang and X. Peng, A two-photon NIR-to-NIR fluorescent probe for imaging hydrogen peroxide in living cells, *Biosens. Bioelectron.*, 2017, **94**, 536–543.

141 R. D. Hanna, Y. Naro, A. Dieters and P. E. Floreancig, Alcohol, Aldehyde, and Ketone Liberation and Intracellular Cargo Release through Peroxide-Mediated α-Boryl Ether Fragmentation, *J. Am. Chem. Soc.*, 2016, **138**, 13353–13360.

142 Z. F. Chen, B. Zhao, X. Y. Tang, W. Li, L. L. Zhu, C. S. Tang, J. B. Du and H. F. Jin, Red yeast rice prevents atherosclerosis through regulating inflammatory signaling pathways, *Chin. Med. J.*, 2011, **124**, 3460–3467.

143 R. Ying, X. Q. Wang, Y. Yang, Z. J. Gu, J. T. Mai, Q. Qiu, Y. X. Chen and J. F. Wang, Hydrogen sulfide suppresses endoplasmic reticulum stress-induced endothelial-to-mesenchymal transition through Src pathway, *Life Sci.*, 2016, **144**, 208–217.

144 W. Shu, S. Zang, C. Wang, M. Gao, J. Jing and X. Zhang, An Endoplasmic Reticulum-Targeted Ratiometric Fluorescent Probe for the Sensing of Hydrogen Sulfide in Living Cells and Zebrafish, *Anal. Chem.*, 2020, **92**, 9982–9988.

145 W. Yu, H. Jin, C. Tang, J. Du and Z. Zhang, Sulfur-containing gaseous signal molecules, ion channels and cardiovascular diseases, *Br. J. Pharmacol.*, 2018, **175**, 1114–1125.

146 M. Niu, Y. Han, Q. Li and J. Zhang, Endogenous sulfur dioxide regulates hippocampal neuron apoptosis in developing epileptic rats and is associated with the PERK signaling pathway, *Neurosci. Lett.*, 2018, **665**, 22–28.

147 Z.-Y. Li, X.-L. Cui, Y.-H. Yan, Q.-L. Che, J.-Y. Miao, B.-X. Zhao and Z.-M. Lin, A novel endoplasmic reticulum-targeted ratiometric fluorescent probe based on FRET for the detection of SO_2 derivatives, *Dyes Pigm.*, 2021, **188**, 109180.

148 J. A. Cotruvo, A. T. Aron, K. M. Ramos-Torres and C. J. Chang, Synthetic fluorescent probes for studying copper in biological systems, *Chem. Soc. Rev.*, 2015, **44**, 4400.

149 H. Hayashi, A. Hattori, Y. Tatsumi, K. Hayashi, Y. Katano, J. Ueyama, S. Wakusawa, M. Yano and H. Goto, Various copper and iron overload patterns in the livers of patients with Wilson disease and idiopathic copper toxicosis, *Med. Mol. Morphol.*, 2013, **46**, 133.

150 S. Y. Park, W. Kim, S.-H. Park, J. Han, J. Lee, C. Kang and M. H. Lee, An endoplasmic reticulum-selective ratiometric fluorescent probe for imaging a copper pool, *Chem. Commun.*, 2017, **53**, 4457–4460.

151 A. Deschamps, A.-S. Colinet, O. Zimmermannova, H. Sychrova and P. Morsomme, A new pH probe localized in the Golgi apparatus of Saccharomyces cerevisiae reveals unexpected roles of Vph1p and Stv1p isoforms, *Sci. Rep.*, 2020, **10**, 1881.

152 M. M. Wu, J. Llopis, S. Adams, J. M. McCaffery, M. S. Kulomaa, T. E. Machen, H.-P. H. Moore and R. Y. Tsien, Organelle pH studies using targeted avidin and fluorescein-biotin, *Chem. Biol.*, 2000, 7, 197.

153 S. Bernales, S. Schuck and P. Walter, ER-phagy: selective autophagy of the endoplasmic reticulum, *Autophagy*, 2007, **3**, 285.

154 R. Sano and J. C. Reed, ER stress-induced cell death mechanisms, *Biochim. Biophys. Acta*, 2013, **1833**, 3460.

155 L. He, B. Dong, Y. Liu and W. Lin, Fluorescent chemoprobes manipulated by dual/triple interplaying sensing mechanisms, *Chem. Soc. Rev.*, 2016, **45**, 6449.

156 M. A. Ruby, J. Massart, D. M. Hunerdosse, M. Schonke, J. C. Correia, S. M. Louie, J. L. Ruas, E. Naslund, D. K. Nomura and J. R. Zierath, Human Carboxylesterase 2 Reverses Obesity-Induced Diacylglycerol Accumulation and Glucose Intolerance, *Cell Rep.*, 2017, **18**, 636–646.

157 Y. Li, M. Zalzala, K. Jadhav, Y. Xu, T. Kasumov, L. Yin and Y. Zhang, Carboxylesterase 2 prevents liver steatosis by modulating lipolysis, endoplasmic reticulum stress, and lipogenesis and is regulated by hepatocyte nuclear factor 4 alpha in mice, *Hepatology*, 2016, **63**, 1860–1874.

158 X. Tian, F. Yan, J. Zheng, X. Cui, L. Feng, S. Li, L. Jin, T. D. James and X. Ma, Endoplasmic Reticulum Targeting Ratiometric Fluorescent Probe for Carboxylesterase 2 Detection in Drug-Induced Acute Liver Injury, *Anal. Chem.*, 2019, **91**, 15840–15845.

159 X. Li, J. Yu, L. Gong, Y. Zhang, S. Dong, J. Shi, C. Li, Y. Li, Y. Zhang and H. Li, Heme oxygenase-1(HO-1) regulates Golgi stress and attenuates endotoxin-induced acute lung injury through hypoxia inducible factor-1α (HIF-1α)/HO-1 signaling pathway, *Free Radical Biol. Med.*, 2021, **165**, 243–253.

160 F. Coceani, L. Kelsey, E. Seidlitz, G. S. Marks, B. E. McLaughlin, H. J. Vreman, D. K. Stevenson, M. Rabinovitch and C. Ackerley, Carbon monoxide formation in the ductus arteriosus in the lamb: implications for the regulation of muscle tone, *Br. J. Pharmacol.*, 1997, **120**, 599–608.

161 X. Wang, Y. Wang, H. P. Kim, K. Nakahira, S. W. Ryter and A. M. K. Choi, Carbon Monoxide Protects against Hyperoxia-induced Endothelial Cell Apoptosis by Inhibiting Reactive Oxygen Species Formation, *J. Biol. Chem.*, 2007, **282**, 1718–1726.

162 H. Wang, Z. He, Y. Yang, J. Zhang, W. Zhang, W. Zhang, P. Li and B. Tang, Ratiometric fluorescence imaging of Golgi H_2O_2 reveals a correlation between Golgi oxidative stress and hypertension, *Chem. Sci.*, 2019, **10**, 10876.

163 S. Seng, Z. Zheng, S. Gong and G. Feng, A unique probe enables labeling cell membrane and Golgi apparatus and tracking peroxynitrite in Golgi oxidative stress and drug-induced liver injury, *Sens. Actuators, B*, 2022, **136**, 131751.

164 Z. Zheng, S. Feng, S. Gong and G. Feng, Golgi-targetable fluorescent probe for ratiometric imaging of CO in cells and zebrafish, *Sens. Actuators, B*, 2021, **347**, 130631.

165 X. Rong, C. Liu, M. Li, H. Zhu, Y. Zhang, M. Su, X. Wang, X. Li, K. Wang, M. Yu, W. Sheng and B. Zhu, An Integrated Fluorescent Probe for Ratiometric Detection of Glutathione in the Golgi Apparatus and Activated Organelle Targeted Therapy, *Anal. Chem.*, 2021, **93**, 16105–16112.

166 S.-S. Wang, S.-Y. Du, X. He, Y.-M. Qi, X.-L. Li, R.-X. Rong, Z.-R. Cao and K.-R. Wang, Nucleus-targeting imaging and

enhanced cytotoxicity based on naphthalimide derivatives, *Bioorg. Chem.*, 2021, **115**, 105188.

167 C.-G. Dai, J.-L. Wang, Y.-L. Fu, H.-P. Zhou and Q.-H. Song, Selective and Real-Time Detection of Nitric Oxide by a Two-Photon Fluorescent Probe in Live Cells and Tissue Slices, *Anal. Chem.*, 2017, **89**, 10511–10519.

168 C. Li, W.-J. Tang, W. Feng, C. Liu and Q.-H. Song, A rapid-response and ratiometric fluorescent probe for nitric oxide: From the mitochondria to the nucleus in live cells, *Anal. Chim. Acta*, 2020, **1096**, 148–158.

169 W. Sun, J.-X. Cui, L.-L. Ma, Z.-L. Lu, B. Gong, L. He and R. Wang, Imaging nucleus viscosity and G-quadruplex DNA in living cells using a nucleus-targeting two-photon fluorescent probe, *Analyst*, 2018, **143**, 5799.

170 K.-N. Wang, L.-Y. Liu, D. Mao, S. Xu, C.-P. Tan, Q. Cao, Z.-W. Mao and B. Liu, A Polarity-Sensitive Ratiometric Fluorescence Probe for Monitoring Changes in Lipid Droplets and Nucleus during Ferroptosis, *Angew. Chem., Int. Ed.*, 2021, **60**, 15095.

171 F. Yang, C. Wang, L. Wang, Z.-W. Ye, X.-B. Song and Y. Xiao, Hoechst-naphthalimide dyad with dual emissions as specific and ratiometric probe for nucleus DNA damage, *Chin. Chem. Lett.*, 2017, **28**, 2019–2022.

172 J. Bucevicius, J. Keller-Findeisen, T. Gilat, S. W. Hell and G. Lukinavicius, Rhodamine–Hoechst positional isomers for highly efficient staining of heterochromatin, *Chem. Sci.*, 2019, **10**, 1962–1970.

173 S. Staubach and F.-G. Hanisch, Lipid rafts: signaling and sorting platforms of cells and their roles in cancer, *Expert Rev. Proteomics*, 2011, **8**, 263–277.

174 P. Sengupta, A. Y. Seo, H. A. Pasolli, Y. E. Song, M. C. Johnson and J. Lippincott-Schwartz, A lipid-based partitioning mechanism for selective incorporation of proteins into membranes of HIV particles, *Nat. Cell Biol.*, 2019, **21**, 452–461.

175 S. T. Yang, A. J. B. Kreutzberger, V. Kiessling, B. K. Ganser-Pornillos, J. M. White and L. K. Tamm, HIV virions sense plasma membrane heterogeneity for cell entry, *Sci. Adv.*, 2017, **3**, 1700338.

176 G. Di Paolo and T. W. Kim, Linking lipids to Alzheimer's disease: cholesterol and beyond, *Nat. Rev. Neurosci.*, 2011, **12**, 284–296.

177 C. L. Schengrund, Lipid rafts: Keys to neurodegeneration, Lipid rafts: Keys to neurodegeneration, *Brain Res. Bull.*, 2010, **82**, 7–17.

178 T. Zhang, L. Li, F. Huo, W. Zhang, J. Chao and C. Yin, Alkyl chain regulated cytomembrane and mitochondria targeting fluorescent probes for ratiometric sensing SO_2 and its bio-application in mice model, *Sens. Actuators, B*, 2021, **342**, 130041.

179 S. Sigismund, S. Confalonieri, A. Ciliberto, S. Polo, G. Scita and P. P. Di Fiore, Endocytosis and signaling: cell logistics shape the eukaryotic cell plan, *Physiol. Rev.*, 2012, **92**, 273–366.

180 J. R. Casey, S. Grinstein and J. Orlowski, Probes and regulators of intracellular pH, *Nat. Rev. Mol. Cell Biol.*, 2010, **11**, 50–61.

181 X. Liu, Y. Su, H. Tian, L. Yang, H. Zhang, X. Song and J. W. Foley, Ratiometric Fluorescent Probe for Lysosomal pH Measurement and Imaging in Living Cells Using Single-Wavelength Excitation, *Anal. Chem.*, 2017, **89**, 7038–7045.

182 S. Michelis, L. Danglot, R. Vauchelles, A. S. Klymchenko and M. Collot, Imaging and Measuring Vesicular Acidification with a Plasma Membrane-Targeted Ratiometric pH Probe, *Anal. Chem.*, 2022, **94**, 5996–6003.

183 X. Kong, J. Yin, M. Li, L. Zhu, B. Dong, Y. Ma and W. Lin, Simultaneously imaging of SO_2 in lysosomes and mitochondria based on a dual organelle-targeted fluorescent probe, *Sens. Actuators, B*, 2019, **292**, 80–87.

184 V. Juvekar, S. J. Park, J. Yoon and H. M. Kim, Recent progress in the two-photon fluorescent probes for metal ions, *Coord. Chem. Rev.*, 2021, **427**, 213574.

185 S. I. Reja, M. Minoshima, Y. Hori and K. Kikuchi, Near-infrared fluorescent probes: a next-generation tool for protein-labeling applications, *Chem. Sci.*, 2021, **12**, 3437.